Through the eye to the brain: Modulating locus coeruleus-mediated arousal via pupil-based neurofeedback

Sarah Nadine Meissner[a]*, Marc Bächinger[a], Sanne Kikkert[a], Jenny Imhof[a], Silvia Missura[a], Manuel Carro Dominguez[a,b] , Nicole Wenderoth[a,b,c]*

[a]Neural Control of Movement Laboratory, Department of Health Sciences and Technology, ETH Zurich, Zurich, Switzerland

[b]Neuroscience Center Zurich, University and ETH Zurich, Winterthurerstrasse 190, 8057 Zurich, Switzerland

[c]Future Health Technologies, Singapore-ETH Centre, Campus for Research Excellence and Technological Enterprise (CREATE), 138602, Singapore.

*Address for correspondence: Sarah Nadine Meissner or Nicole Wenderoth, Neural Control of Movement Laboratory, Department of Health Sciences and Technology, ETH Zurich, Technoparkstrasse 1, 8005 Zurich, Switzerland, Email: sarah.meissner@hest.ethz.ch, nicole.wenderoth@hest.ethz.ch

Keywords: pupillometry, neurofeedback, arousal, locus coeruleus, noradrenaline, self-regulation, fMRI, oddball

Abstract

The brain's arousal state is controlled by several neuromodulatory nuclei known to substantially influence cognition and mental well-being. Here, we investigate whether human participants can gain volitional control of this arousal state using a new pupil-based neurofeedback approach that targets the locus coeruleus (LC), a key regulator of arousal and autonomic function. Our approach inverts the mechanism that LC causally drives pupil dynamics if light conditions are controlled. We show that pupil-based neurofeedback enables participants to acquire volitional control of pupil size. Applying pupil self-regulation systematically modulates activity of the LC and other structures involved in arousal control. Further, it modulates cardiovascular measures such as heart rate, and behavioural and psychophysiological responses during an oddball task closely linked to LC activity dynamics. We provide evidence that pupil-based neurofeedback makes the brain's arousal system accessible to volitional control, a finding that has tremendous potential for translation to behavioral and clinical applications across various domains, including stress-related and anxiety disorders.

Introduction

The brain's arousal state is controlled by several key neuromodulatory nuclei including the noradrenergic (NA) locus coeruleus (LC), the dopaminergic substantia nigra/ventral tegmental area (SN/VTA), the serotonergic dorsal raphe nucleus (DRN), and the cholinergic nucleus basalis of Meynert (NBM)[1–4]. The LC in particular has received increasing attention in the context of arousal regulation[2,5,6]. Serving as the main source of NA to the brain and projecting to various cortical and subcortical brain regions, the LC exerts powerful effects on neural processing[6,7]. Additionally, LC activity modulates cardiovascular function[8] via its projections to autonomic control structures in the brainstem and spinal cord[9].

Theories predominantly based on intracranial recordings in animals suggest that the LC-NA system modulates functional circuits related to wakefulness and sleep[5,9–12] and cognitive processes relevant for task engagement and optimization of task performance[4,7,9,13,14]. These theories postulate that LC neurons exhibit tonic and phasic discharge patterns. Tonic activity is thought to be closely correlated with the general arousal state of the brain (i.e., high tonic LC activity is associated with high arousal), whereas phasic discharge is proposed to facilitate behavioral responses to task-relevant events[4]. Probing these task-relevant processes, often via a two-stimulus oddball paradigm, revealed that phasic LC responses are heavily dependent on the tonic activity level. For instance, recordings in monkeys showed that elevated tonic LC activity was associated with decreased phasic activity in response to oddball stimuli and declines in task performance[15–18].

A growing body of research indicates that, under constant lighting conditions, the eye's pupil size is an indirect 'indicator' of the brain's arousal state. Arousal-related neuromodulatory systems have been directly or indirectly linked to these non-luminance-related changes in pupil size[19–21], however, the strongest evidence indicates that the LC-NA system is implicated in pupil control[21–25]: Selective chemogenetic or optogenetic activation of the LC causes substantial pupil dilation in mice[25–27]. Even though a direct comparison of cholinergic and noradrenergic systems and their role in pupil dynamics in rodents provides evidence for the involvement of both systems, only prolonged pupil dilations during movement were accompanied by sustained cholinergic activity, while moment-to-moment pupil fluctuations during rest closely tracked noradrenergic activity[21]. Furthermore, noradrenergic activity has been observed to precede cholinergic activity relative to peak pupil size[21] and can depolarize cholinergic neurons[1], making it possible that noradrenergic activity drives cholinergic activation. In humans, it has been demonstrated that LC activity measured by functional magnetic resonance imaging (fMRI) correlates with pupil size, both at rest and during various tasks including the oddball paradigm[20,22,23,28].

To date, regulating LC-mediated arousal is challenging and existing approaches in humans are mainly limited to pharmacological agents that often cause pronounced side-effects. Here, we investigated an

alternative approach that seeks to exploit the mechanistic link between LC-NA-mediated arousal and pupil via a novel pupil-based neurofeedback approach (pupil-NF). So far, only a few studies have trained volunteers to self-regulate pupil size with varying degrees of success[29–32]. Volitional pupil size downregulation is especially difficult to acquire[32]. The main idea of our approach is that participants apply different arousing or relaxing mental strategies while receiving quasi-online pupil-NF (Figure 1A). We hypothesized that (i) this type of pupil-NF would allow them to discover suitable mental strategies for volitional up- versus downregulation of pupil size and (ii) such self-regulation is associated with up- versus downregulating activity in LC and other areas strongly involved in arousal control. We further hypothesized that self-regulating LC activity will (iii) modulate stimulus detection behavior during an oddball task shown to depend on LC-NA activity and (iv) cause systematic changes in cardiovascular parameters.

Numerous studies have shown that providing feedback on specific body functions via neuro- or biofeedback enables humans to gain remarkable control over these functions[33–36]. The effectiveness of self-regulation critically depends on whether participants can acquire a suitable mental strategy. Neurofeedback has been shown to facilitate this process[33,36]. Using our new pupil-NF training regime, we show that healthy volunteers can learn to volitionally up- and downregulate their pupil size (Experiments 1AB). Crucially, by combining pupil self-regulation with fMRI and cardiovascular measurements, we show that up- versus downregulating pupil size systematically modulates (i) activity of LC and (interconnected) cortical and subcortical brain regions, including the SN/VTA (Experiment 2) and (ii) heart rate (Experiments 1B,2). Finally, we demonstrate that self-regulating pupil size modulates behavioral performance and psychophysiological markers of LC-NA activity during an auditory oddball task (Experiment 3).

Results

Experiment 1: Pupil-NF training enables healthy volunteers to volitionally regulate pupil size

Healthy participants were randomly assigned to either a pupil-NF (n = 28) or control group (n = 28) and participated in three days of pupil-NF training (Experiment 1A). Prior to training, all participants received instructions on mental strategies derived from previous research[29,32,37–39], such as imagining emotional (i.e., fearful or joyful) situations to upregulate pupil size (UP); or relaxing, safe situations together with focusing on their body and breathing to downregulate pupil size (DOWN; see Supplementary Table (ST) 1 for applied strategies). They participated in three sessions on three separate days (Figure 1B), each consisting of 30 UP and 30 DOWN trials which required them to self-regulate pupil for 15s (Figure 1C, lower panel). Participants of the pupil-NF group received isoluminant visual feedback on pupil size in quasi real-time during regulation and average performance

feedback after regulation (post-trial feedback; Figure 1C, upper panel). Participants of the control group saw matched visual information on the screen but did not receive veridical feedback. At the end of day 3, all participants underwent an additional *no feedback-session* (20 UP and 20 DOWN trials) during which they used the same self-regulation strategies as during training, but without receiving feedback.

Participants of both groups (n = 27 in each group for final analyses) were able to upregulate pupil size (Figure 2A), but the amount of upregulation was substantially larger in the pupil-NF than in the control group. The ability to downregulate pupil became gradually more successful during training in the pupil-NF group while this ability was strongly reduced in the control group (Figure 2B). Importantly, the pupil-NF participants maintained their self-regulation abilities during *no-feedback-trials* at the end of the training, indicating that they acquired a transferable skill that, once learned, can be applied without the need for constant feedback (Figure 2AB; grey lines).

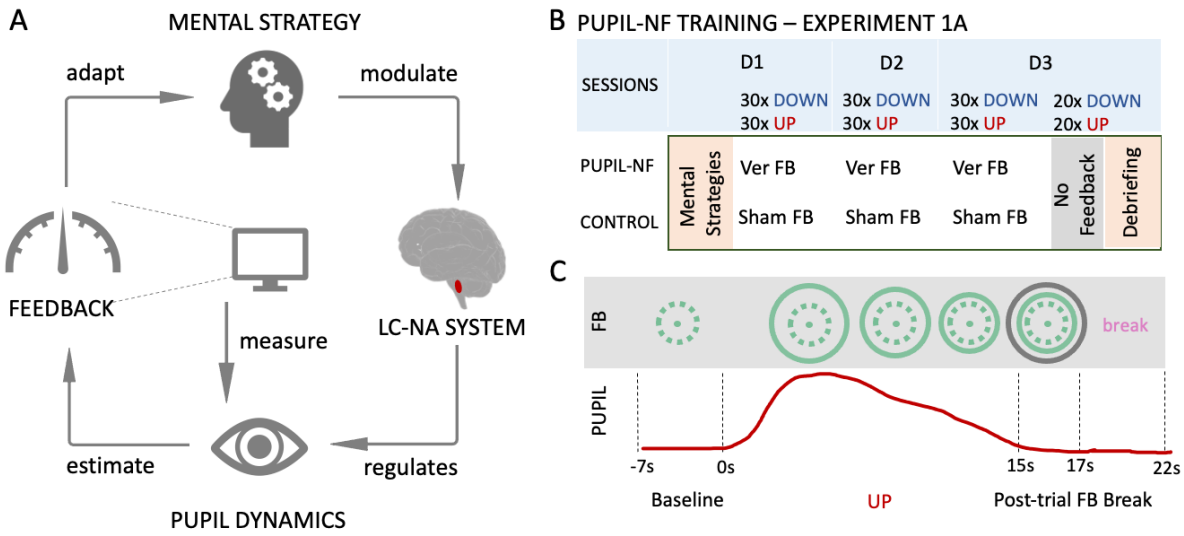

Figure 1. Pupil-based neurofeedback (pupil-NF) training. **A.** Participants apply mental strategies which are believed to modulate arousal via the LC-NA system. Pupil size is measured by an eye tracker and fed back to the participant via an isoluminant visual display **B.** In Experiment 1A, healthy volunteers were informed about potential mental strategies of arousal regulation and then participated in 3 days (D1, D2, D3) of upregulation (UP) and downregulation (DOWN) training (30 trials each) while receiving either veridical (ver) pupil feedback (pupil-NF group) or visually matched sham feedback (control group). At the end of day 3, all participants performed 20 UP and DOWN trials without receiving any feedback and were debriefed on which strategies they have used. **C.** Example trial of the experiment. Each trial consisted of (i) 7s baseline measurements, (ii) 15s modulation phase where the pupil-NF group sees a circle that dynamically changes its diameter as function of pupil size (veridical feedback), (iii) 2s of color-coded post-trial performance feedback (green = average circle size during modulation; black = maximum (UP) or minimum (DOWN) circle size during modulation), and (iv) 5s break. While the upper panel shows an example of what participants would see on their screen, the red line in

the lower panel indicates measured pupil size. Note that the control group (sham feedback) sees a circle that changes independently of pupil size but resembles that of a participant in the pupil-NF group.

Pupil self-regulation was quantified by calculating a pupil modulation index (UP–DOWN; i.e., the difference between pupil diameter changes in the two conditions) which was significantly larger in the pupil-NF than in the control group (Figure 2C; $F(1,21.58) = 21.49$; $p = 0.001$, $\eta_p^2 = 0.50$). A control analysis confirmed that these group differences were driven by volitional pupil modulation and not by differences in absolute pupil size at baseline (all $p \geq 0.49$; Supplementary Figure (SF) 1A).

Next, we conceptually replicated these results in an independent pupil-NF cohort (Experiment 1B). 26 participants (n = 25 for final analyses) followed a similar 3-day training protocol but participated in a no-feedback-session *before* (Pre) and *after* (Post) training (SF 2AB). We calculated a modulation index time series (UP–DOWN) and found that pupil-NF training resulted in significantly higher modulation indices Post as compared to Pre during most of the modulation phase (significant differences: 2.9s – 15s after modulation onset; all $p < 0.049$; Bonferroni corrected, Figure 2D; for condition effect, see SF 2D). This indicates that participants significantly improved their ability to volitionally modulate pupil size after pupil-NF training.

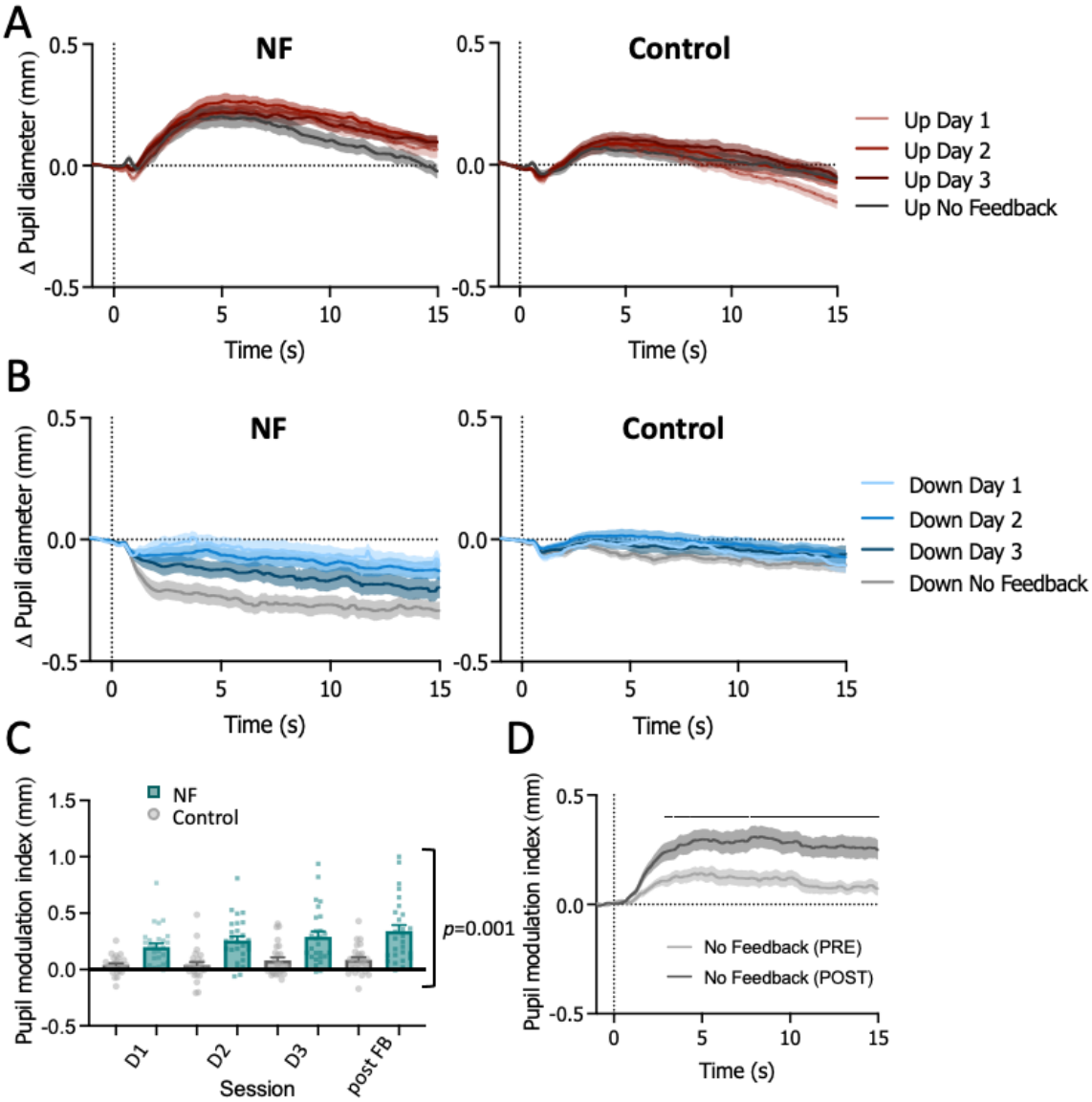

Figure 2. Average changes in pupil size during 15s upregulation (UP) **(A)** and downregulation (DOWN) **(B)** are shown for the pupil-NF (n = 27) and control (n = 27) groups for training sessions on Day 1, Day 2, Day 3, and the no feedback post training session of Experiment 1A. **C.** The pupil modulation index reflects the difference between the average pupil size during the two conditions (UP–DOWN) and is shown for each session (Day 1, Day 2, Day 3, no feedback post training session) and group (control versus pupil-NF group of Experiment 1A; dots and squares represent individual participants). Pupil modulation indices were generally higher in the pupil-NF group compared to the control group (robust ANOVA, main effect of *group*: $F(1,21.58) = 21.49$; $p = 0.001, \eta_p^2 = 0.50$; other main effects/interaction $p \geq 0.07$). **D.** Time series of pupil modulation index measured during the no feedback session before (Pre, light grey) and after pupil-NF training (Post, dark grey) in Experiment 1B (independent cohort, n = 25). Solid black lines at the top indicate clusters of significantly higher modulation indices at Post compared to Pre (SPM1D repeated measures ANOVA; all $p < 0.05$; Bonferroni-corrected). Shaded areas and error bars indicate SEM.

Our results from Experiments 1AB show that healthy volunteers can learn to volitionally modulate pupil size. Importantly, substantial differences in self-regulation capabilities between (i) pupil-NF and

sham feedback and (ii) Pre versus Post performance in a separate pupil-NF cohort indicates that neurofeedback significantly improves volitional pupil diameter control.

Experiment 2: Combining self-regulation of pupil size with simultaneous fMRI

Previous studies have repeatedly linked non-luminance-mediated pupil size changes to activity changes in arousal-regulating centers including the LC[20,22–25]. Here, we tested the hypothesis that self-regulating pupil size is associated with activity changes in the LC and other regions involved in arousal regulation. 25 trained participants from the pupil-NF groups in Experiments 1AB performed pupil up- versus downregulation during two fMRI sessions, one measuring activity across the whole brain, and one specifically measuring brainstem activity (order of sessions was counterbalanced). Participants performed 15s of pupil size modulation and received post-trial performance feedback. Pupillometry data confirmed that participants were able to self-regulate pupil size (Figures 3A, 4A).

Self-regulation of pupil size is linked to changes in LC activity and other arousal-regulating brainstem regions

Based on previous findings, we predefined the LC, DRN, NBM, and SN/VTA as regions of interest (ROI) since these nuclei are known to substantially contribute to arousal control[1–4]. Additionally, the LC, NBM and DRN have been linked to pupil size changes[19,21,40]. However, whether the NBM and DRN modulate pupil size directly or via the LC-NA system is still an ongoing debate. Anatomically, the size of the pupil is controlled by the tone of (i) the dilator pupillae muscle receiving innervation via noradrenergic sympathetic neurons and (ii) the constrictor pupillae muscle receiving innervation via cholinergic parasympathetic neurons[9]. Thus, pupil diameter reflects the relative activity of these opposing outputs of the autonomic nervous system[6,9]. There is growing consensus that the LC modulates pupil by (i) facilitating sympathetic activity via projections to the intermediolateral (IML) cell column of the spinal cord, and (ii) inhibiting parasympathetic activity via its projections to the Edinger-Westphal nucleus (EWN)([6,9] reviewed in[40]). Another important candidate controlling non-luminance-related pupil responses, particularly during the integration of multisensory input and orienting responses, is the superior colliculus (SC)[24,40]. It is assumed that the SC modulates pupil control through projections (i) to the EWN directly and indirectly via the mesencephalic cuneiform nucleus (MCN), influencing parasympathetic activity, and (ii) to the IML via the MCN, influencing sympathetic activity[40]. Therefore, we added the SC as an additional control ROI to our analysis (Figure 3F).

After applying rigorous pre-processing steps to remove physiological noise from brainstem data, we extracted the mean signal intensity during UP>rest and DOWN>rest from the LC, SN/VTA, DRN, NBM, and SC (n = 22). As hypothesized, we observed that pupil upregulation was associated with significantly higher LC activation than downregulation ($Z = 3.0$, $p = 0.015$, $r = 0.64$). Similar results

were found for the SN/VTA (Z = 2.90, p = 0.016, r = 0.62) and a trend was observed for the NBM (Z = 2.26, p = 0.072, r = 0.48; p-values are sequential Bonferroni-corrected[41]; Figure 3B). Activation differences in all other ROIs failed to reach significance ($p \geq 0.32$; additional post-hoc Bayesian analyses revealed moderate evidence for the null hypothesis: UP = DOWN, Bayesian paired samples t-tests SC: BF10 = 0.34; DRN: BF10 = 0.31).

We further investigated whether pupil size modulations throughout the fMRI runs correlated with continuous BOLD activity changes in the pre-defined ROIs and found a significant association in the SN/VTA (Z = 3.72, p = 0.005, r = 0.79) and observed – after correction for multiple comparisons – a trend in the LC and NBM (LC: Z = 2.22, p = 0.078, r = 0.47; NBM: Z = 2.39; p = 0.068, r = 0.51) but not in the DRN or SC (all $p \geq 0.16$; Figure 3C).

Next, we complemented our a-priori-defined ROI analysis with an exploratory, data-driven approach considering activity changes for UP>DOWN across the brainstem. Given the limited signal-to-noise ratio for brainstem responses and our strict pre-processing pipeline, we report all voxels $p < 0.05$ without applying corrections for multiple comparisons[28]. In line with our ROI analyses, we identified significant bilateral activation in the LC (Figure 3D, upper panel), SN, VTA, NBM and small activity clusters overlaying the SC and DRN (Figure 3E, upper panel). Furthermore, pupil upregulation activated several brainstem nuclei involved in arousal and autonomic regulation[42–48] such as the pedunculopontine nucleus and the periaqueductal gray (ST 2A; for DOWN>UP results, see SF 3A).

We also exploratively correlated continuous pupil diameter with continuous BOLD activity changes for every voxel in the brainstem. In line with our ROI results, we found a significant correlation between pupil size and BOLD activity in the LC (Figure 3D, lower panel), SN, VTA, NBM, and a small overlap with the DRN (Figure 3E, lower panel). Additionally, pupil size was found to correlate with activity in brainstem regions involved in arousal and autonomic regulation[42–48] similar to the UP>DOWN contrast (all voxels reaching significance at $p < 0.05$ uncorrected[28]; ST 2B).

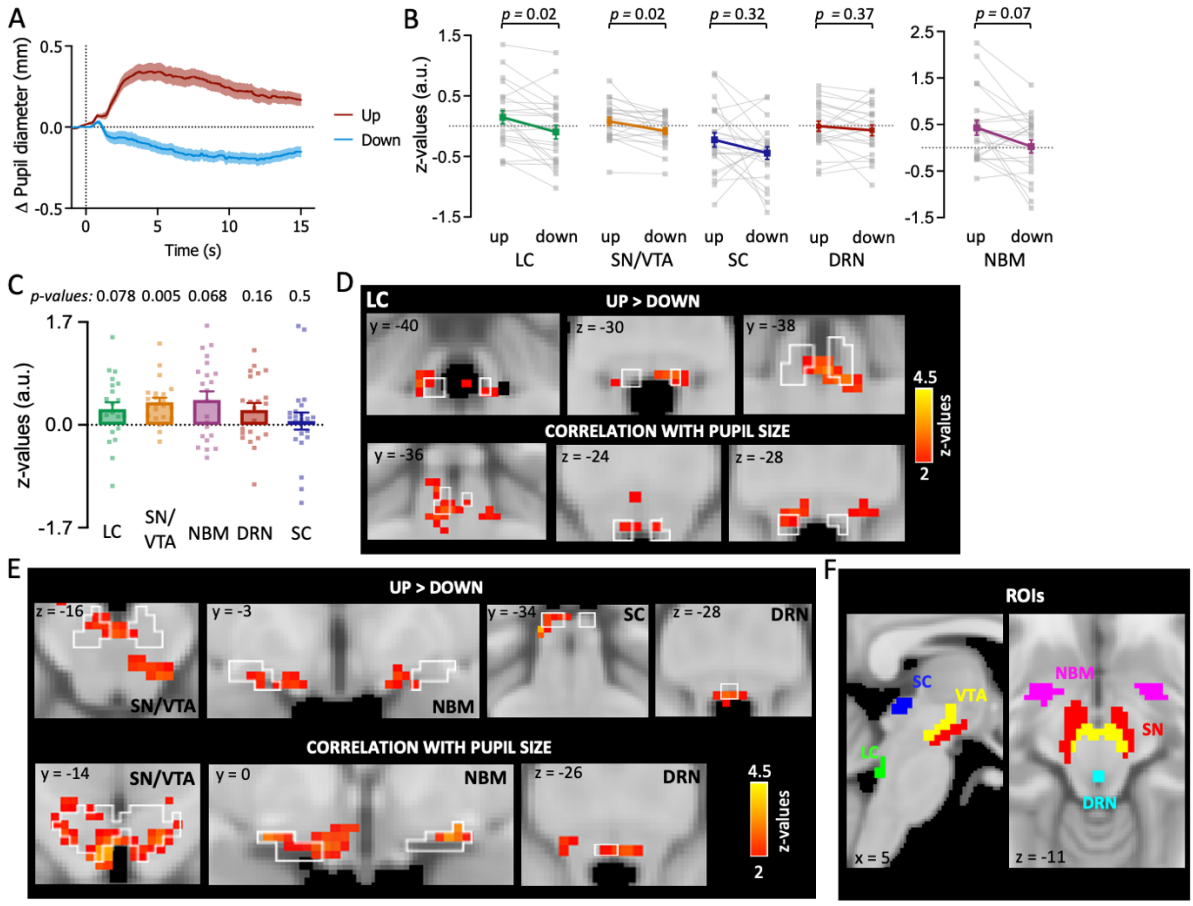

Figure 3. Brainstem fMRI session. **A.** Changes in pupil size averaged across all participants for UP (red) and DOWN (blue) trials showing successful self-regulation of pupil size during brainstem fMRI recording. **B.** Activity during UP versus DOWN phases of pupil self-regulation in the different regions of interest (ROIs). Statistical comparisons using Wilcoxon Signed Rank tests revealed significant effects (UP > DOWN) in the LC, the SN/VTA, and the NBM (trend-level), but not in the SC and DRN. **C.** Correlation between continuous pupil size changes and BOLD response changes shown as z-values for the different ROIs. Statistical comparison (against 0) revealed significant effects for the SN/VTA and a trend for the LC and the NBM. All ROI analyses in **B** and **C** were corrected for multiple comparisons using sequential Bonferroni correction. Squares represent individual data **D. Upper panel:** Data-driven analysis across the brainstem revealed a significant bilateral activation cluster in the LC during pupil upregulation (UP > DOWN; $p < 0.05$, uncorrected; upper panel). **Lower panel:** Correlation analysis revealed that BOLD activity at the LC covaries with continuous changes in pupil diameter ($p < 0.05$, uncorrected). **E. Upper panel:** Other brainstem areas than LC were identified by the data-driven analysis when comparing UP > DOWN regulation of pupil size. Significant clusters ($p < 0.05$, uncorrected) were found in SN/VTA, NBM, and small parts of the SC and DRN. **Lower panel:** The same areas – except for the SC – exhibited a significant correlation between changes in pupil diameter and BOLD activity (lower panel; $p < 0.05$, uncorrected). The white outlines in **D** and **E** indicate different brainstem[42–48] and basal forebrain regions[49]. **F.** A-priori defined ROIs in the brainstem[42–48] and basal forebrain[49] in MNI space. Shaded areas and error bars indicate SEM. Locus coeruleus (LC); substantia nigra (SN) and ventral tegmental area (VTA) combined into one ROI (SN/VTA); dorsal raphe nucleus (DRN); nucleus basalis of Meynert (NBM); and superior colliculus (SC).

In summary, our brainstem fMRI analyses revealed that pupil self-regulation is indeed linked to LC activity changes driven by activation during upregulation and deactivation during downregulation. Not surprisingly, the LC is not the only area modulated by pupil self-regulation; we also identified other brainstem regions known to be involved in arousal and autonomic regulation. This finding is important because it shows that the mechanism that LC activity drives pupil size can be inverted in the context of pupil-NF, thereby making the brain's arousal system accessible to voluntary control.

Self-regulation of pupil size is linked to changes in cortical and subcortical regions closely connected with the LC

To investigate the effects of pupil self-regulation on a wide range of cortical and subcortical structures, we analyzed whole-brain fMRI data (n = 24). Contrasting UP>DOWN phases, we found that upregulation was associated with significantly more activation in various brain regions known to be closely connected to the LC, most notably in the dorsal anterior cingulate cortex (dACC), paracingulate gyrus (PCG), dorsolateral prefrontal cortex (DLPFC), orbitofrontal cortex (OFC), precuneus and thalamus (Figure 4CD; ST 3A). Additionally, we observed significant activation in primary somatosensory regions (SM1), the basal ganglia (globus pallidus, caudate nucleus), and cerebellum (Figure 4CD).

Next, we investigated in which brain areas BOLD activity covaried with pupil size throughout the task and observed significant effects in the dACC, thalamus, globus pallidus, and cerebellum (Figure 4B; ST 4), partially overlapping with regions significantly activated during upregulation of pupil size (UP>DOWN; for DOWN>UP results, see SF 3BC and ST 3B).

Our whole-brain fMRI data indicates that pupil self-regulation is linked to an interplay of activation and deactivation in a number of circumscribed brain regions including prefrontal, parietal, thalamic and cerebellar areas strongly interconnected with the LC.

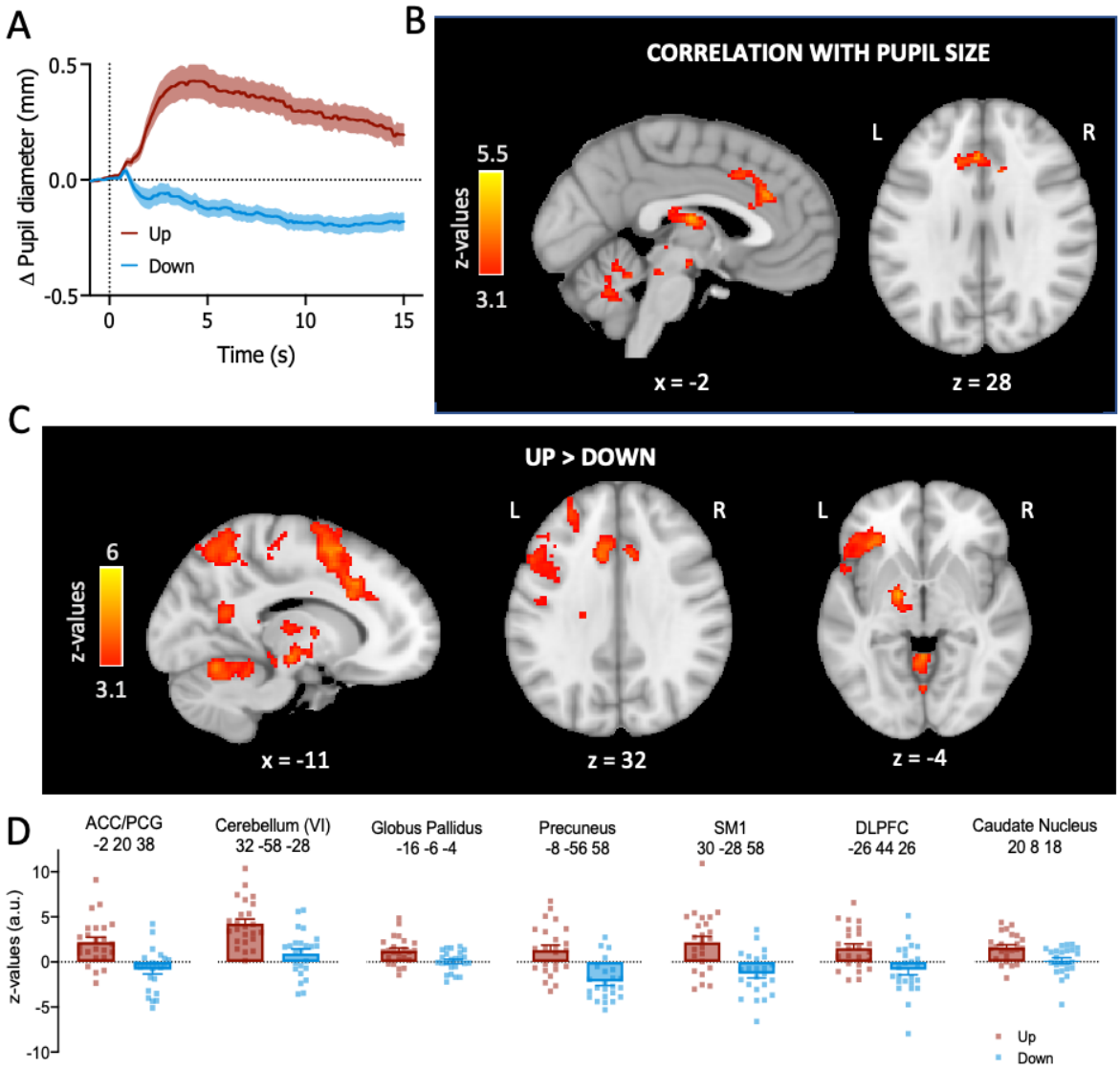

Figure 4. Whole-brain fMRI results. **A.** Changes in pupil size averaged across all participants for UP (red) and DOWN (blue) trials showing successful self-regulation of pupil size during whole-brain fMRI recordings. **B.** Whole-brain maps showing brain regions where BOLD activity correlates with pupil size changes throughout the run **C.** Whole-brain maps depicting brain regions that showed a significant activation during UP as compared to DOWN. All activation maps in **(B)** and **(C)** are thresholded at Z > 3.1 and FWE-corrected using a cluster significance level of $p < 0.05$. **D.** Estimated BOLD response represented by z-values for UP vs rest and DOWN vs rest extracted from the peak voxel of each significant cluster shown in C. Squares indicate individual participants. Shaded areas and error bars indicate SEM.

Self-regulation of pupil size modulates cardiovascular parameters

We tested whether self-regulating pupil size influenced cardiovascular parameters by analyzing electrocardiogram (ECG) signals recorded in 15 participants during pupil-NF training (Experiment 1B) and pulse oximetry data recorded during the subsequent fMRI sessions (Experiment 2). Generally, we observed higher heart rates during UP as compared to DOWN trials (Figure 5AC). This difference became increasingly pronounced throughout pupil-NF training (*condition***session* interaction; $F(2.35,$

32.89) = 3.98, p = 0.023, η_p^2 = 0.22) and remained stable post-training during fMRI (main effect *condition*; $F(1,22) = 72.25$, $p < 0.001$, $\eta_p^2 = 0.77$; Figure 5AC). We further showed that pupil diameter and heart rate changes were largely unrelated prior to pupil-NF training ($p > 0.5$, Figure 5E, left panel) but exhibited a significant positive correlation during fMRI where a higher pupil modulation index (UP–DOWN), thus better pupil self-regulation, was associated with larger differences in heart rate (UP–DOWN; rho = 0.63; p = 0.002; sequential Bonferroni-corrected; Figure 5E, right panel).

We also calculated the root mean square of successive differences (RMSSD), a heart rate variability (HRV) measure suggested to represent a marker of parasympathetic activity. There was no clear effect of pupil self-regulation training on HRV (all $p > 0.34$; left panel, Figure 5BD) and pupil diameter changes were largely unrelated to HRV changes prior to and following training during fMRI (all $p > 0.2$, Figure 5F). During the fMRI sessions, HRV was generally higher during pupil down- than upregulation, however, these differences only tended to be significant (brainstem: Z = 1.71, p = 0.086, r = 0.35; whole-brain: Z = 1.91; p = 0.056, r = 0.39; right panel, Figure 5BD).

Taken together, pupil self-regulation following pupil-NF training modulated cardiovascular parameters, particularly heart rate, which is in line with the model that LC modulates autonomic function.

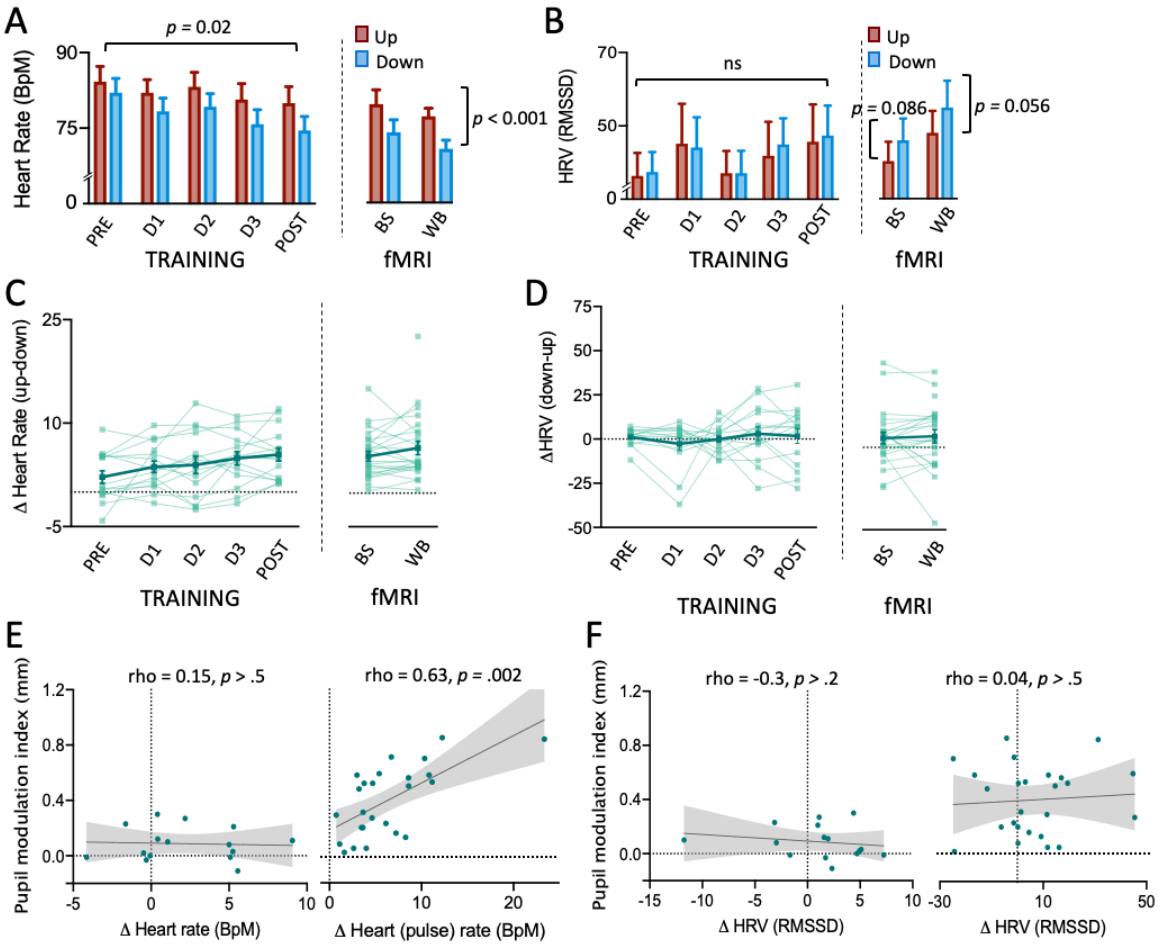

Figure 5. Effects of pupil self-regulation on cardiovascular parameters. Heart rate **(A)** and heart rate variability (HRV) **(B)** averaged for UP and DOWN trials across all participants for pupil-NF training (n = 15, left panel) and fMRI sessions (n = 24, right panel). HRV was estimated as the root mean square of successive differences (RMSSD). Self-regulation of pupil size systematically modulated heart rate with an increasingly larger difference between UP and DOWN trials over training sessions (repeated measures ANOVA: *condition*session* interaction: $F(2.35, 32.89) = 3.98$, $p = 0.023$, $\eta_p^2 = 0.22$; Greenhouse-Geisser-corrected) which remained stable after training during fMRI (repeated measures ANOVA; main effect *condition;* $F(1,22) = 72.25$, $p < 0.001$, $\eta_p^2 = 0.77$). Self-regulation did not significantly modulate HRV during training (robust ANOVA: $p > 0.34$). After training during fMRI, we observed a trend towards higher HRV during DOWN compared to UP (Wilcoxon Signed Rank Test; brainstem session: $p = 0.086$; whole-brain session: $p = 0.056$). **C.** and **D.** show individual differences in heart rate (UP-DOWN differences) and RMSSD (DOWN-UP differences) for training (left panels) and fMRI sessions (right panel). The thick solid line represents the group average, thin lines represent individual data. **E.** Spearman rho correlation coefficients between pupil modulation indices (i.e., the difference between pupil diameter changes in the two conditions; UP-DOWN) and differences in heart rate (UP-DOWN) revealing a significant link following (right panel; during fMRI) but not prior to pupil-NF training (left panel) **F.** Non-significant Spearman rho correlation coefficients between pupil modulation indeces (UP-DOWN) and RMSSD differences (DOWN-UP) prior to (left panel) and after pupil-NF training during fMRI (right panel). Error bars indicate SEM. The grey shading (**E** and **F)** around the solid line represents the 95% confidence interval around the line of best fit. BS = brainstem fMRI; WB = whole-brain fMRI.

Experiment 3: Combining self-regulation of pupil size with an auditory oddball task

To determine whether self-regulation of pupil size further impacts behavioral measures and psychophysiological markers of LC-NA activity, we combined our pupil-NF approach with an auditory oddball task (Figure 6A) for which the detection of salient target stimuli has been linked to phasic LC activity[15]. 22 participants that underwent pupil-NF training (Experiments 1AB) performed an oddball task while (i) upregulating pupil size (ii) downregulating pupil size or (iii) executing a cognitive control task which required them to silently count backwards in steps of seven. The latter condition was included to control for effects of cognitive effort that may arise from executing pupil-self regulation simultaneously with the oddball task.

Participants (n = 20 for final analyses) were able to successfully self-regulate pupil size (main effect *condition*: $F(1.52,16.67) = 9.33$, $p = 0.003$, $\eta_p^2 = 0.46$; Figure 6BC) as indicated by smaller (baseline-corrected) pupil sizes during DOWN than UP and control trials, even when simultaneously performing the oddball task. Also, absolute size was increased for UP as compared to DOWN trials only during self-regulation but not during the baseline phase (SF 1C and 4).

Unexpectedly, absolute pupil size was increased for control trials (SF 1C and 4). Since this increase was observed during the baseline *and* self-regulation phase, (baseline-corrected) pupil sizes were at intermediate levels compared to the UP and DOWN condition (Figure 6B). This suggest that the counting task had a potentially higher cognitive load than pupil self-regulation which was, however, consistently increased throughout all phases of the control condition.

Self-regulation of pupil size modulates psychophysiological markers of LC activity

Previous research in monkeys suggests that elevated tonic LC activity levels constrain the intensity of phasic LC activity in response to salient stimuli[16–18]. Here, we tested the prediction that phasic activity varies depending on levels of tonic activity. We particularly investigated whether sustained volitional pupil size modulation impacts pupil dilation responses to target sounds during the simultaneously performed oddball task, which has been linked to phasic LC activity. In line with previous literature, we observed that pupil self-regulation led to differences in pupil dilation responses to target sounds ($z^* = 7.29$; 714-3000ms, $p < 0.001$, Figure 6D, left panel) with significantly larger initial pupil dilation and prolonged elevated dilation levels during DOWN compared to UP trials ($z^* = 4.07$; 718-2669ms, $p < 0.001$; 2851-3000ms, $p = 0.005$, Bonferroni-corrected).

The cognitive control and UP condition caused a similar initial pupil dilation but the time course after peak dilation differed significantly between these conditions ($z^* = 4.12$; between 1381ms-3000ms, all $p \leq 0.02$; Bonferroni-corrected, Figure 6D, left panel). Differences between control and DOWN trials did not reach significance. Finally, we tested whether there is a systematic relationship between

baseline pupil size and phasic pupil dilation. We found that smaller baseline pupil sizes before target onset were significantly correlated with larger pupil dilation responses towards the target sound (r_{rm} = -0.28, $p < 0.001$; Figure 6F, left panel; for correlations within conditions, see SF 5A).

Standard tones evoked only a minor pupil response (Figure 6D, right panel). Responses differed significantly between conditions mainly driven by prolonged elevation of pupil size in UP compared to DOWN trials ($z^* = 3.93$: 1081-2251ms, $p < 0.001$; Bonferroni-corrected) and a faster decrease in pupil size in DOWN compared to control trials ($z^* = 4.23$, between 916-1233ms, all $p \leq 0.02$; Bonferroni-corrected). However, these differences were only observed *after* peak dilation and likely reflect the effects of self-regulation on measured pupil size.

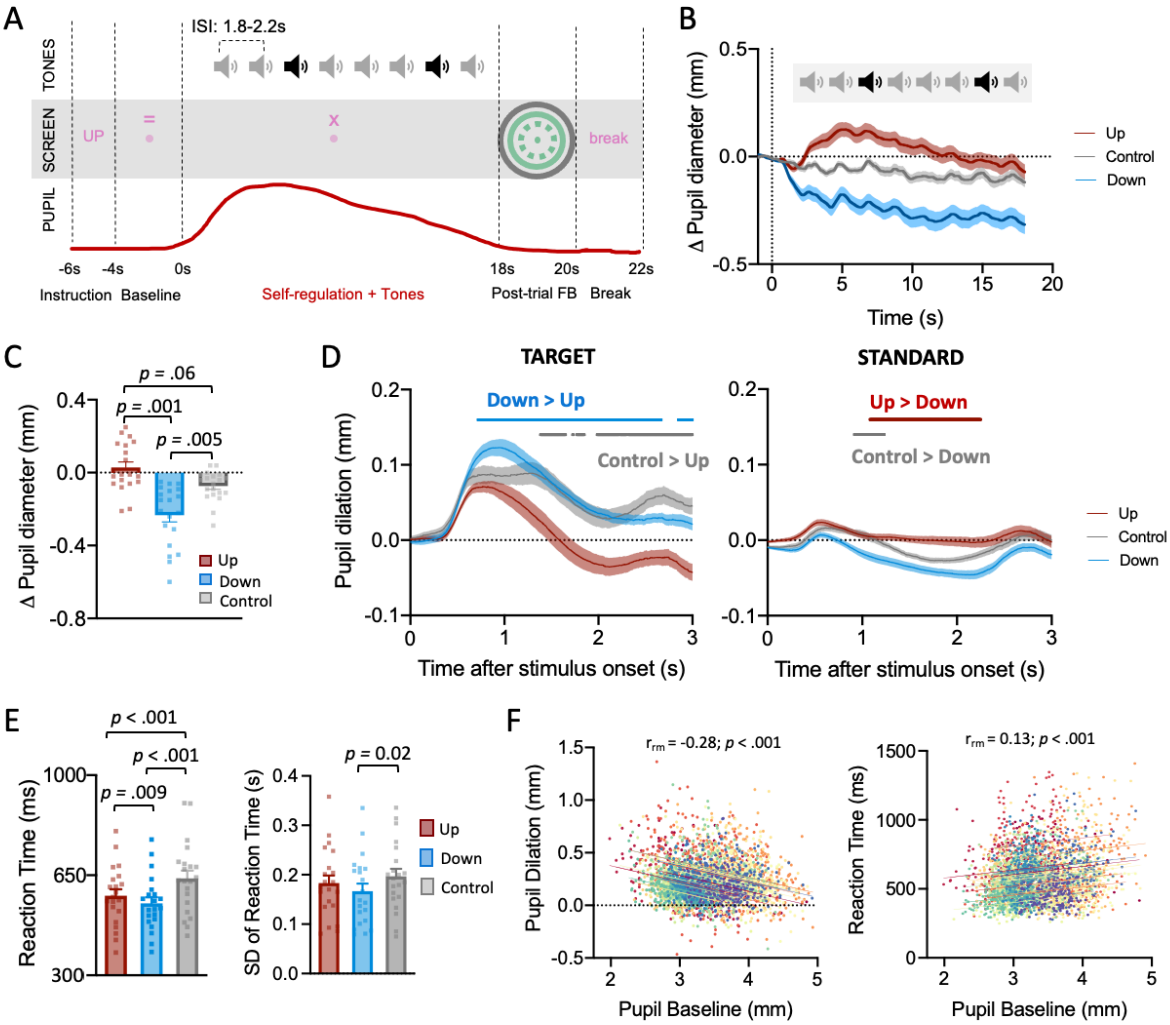

Figure 6. Self-regulation of pupil size combined with an auditory oddball task. **A.** Schematic depiction of an example trial (UP) of Experiment 3 combining pupil-NF and the oddball task in which participants reacted to target tones (black sound icon) by button press and ignored standard tones (grey sound icon) while simultaneously up- or downregulating pupil size or counting backwards (i.e., control). **B.** Pupil size changes averaged across participants for UP (red), DOWN (blue) and control trials (grey, counting backwards in steps of 7) showing the last second of the baseline phase as well as the complete modulation phase of 18s for 20

participants. **C.** Pupil size changes during the modulation phase from baseline (last 1s of baseline phase) averaged across the respective condition and participants showing significantly lower values in DOWN as compared to control and UP trials (robust repeated measures ANOVA with the factor *condition:* $F(1.52,16.67) = 9.33$, $p = 0.003$, $\eta_p^2 = 046$; DOWN vs. UP: $\hat{\psi} = -0.23$; $p = 0.001$; DOWN vs. control: $\hat{\psi} = -0.14$; $p = 0.005$; for UP vs. control we only found a trend-level effect: $\hat{\psi} = 0.10$; $p = .06$). **D.** Baseline-corrected pupil dilation responses evoked by target (left) and standard tones (right) for UP, DOWN and control trials. Solid lines above the dilation time series indicate time windows of significantly smaller responses to targets in UP as compared to DOWN (blue) and control trials (grey; left panel) and significantly larger responses to standard tones in UP (red) and control (grey) than in DOWN trials (right panel; all tests are Bonferroni-corrected post-hoc tests of SPM1D repeated measures ANOVA with the factor *condition;* all $p < 0.05$) **E.** Behavioral performance of 21 participants during the oddball task depicting faster responses during DOWN as compared to UP (repeated measures ANOVA main effect *condition*: $F(2,40) = 35.97$, $p < 0.001$, $\eta_p^2 = 0.64$, DOWN versus UP: $t(20) = -2.87$, p = 0.009, d = 0.63) and control trials (DOWN versus control: $t(20) = -7.19$, $p < 0.001$, d = 1.57; UP versus control: $t(20) = -6.04$, $p < 0.001$, d = 1.32; left panel; all sequential Bonferroni-corrected). Responses were also less variable (right panel) in DOWN as compared to control trials ($t(20) = -3.01$, $p = 0.02$, d = 0.66; sequential Bonferroni-corrected post-hoc tests of repeated measures ANOVA on reaction time and SD of reaction times with the factor *condition*). **F.** Results of repeated measures correlations between baseline pupil size (500ms prior to target onset) with pupil dilation responses (left panel) and reaction times (right panel) towards targets. Please note that sound icons in **A.** and **B.** indicate standards (grey) and targets (black) played during pupil self-regulation or control trials. Squares in **C.** and **E.** represent individual data. Error bars and shaded areas indicate SEM.

Self-regulation of pupil size modulates oddball task performance

LC activity during the oddball task has been linked to the detection of task-relevant target stimuli[15,17,22,50]. Here, we tested the hypothesis that self-regulation of pupil size modulating LC activity influences behavioral performance during the oddball task. In general, task performance was high (correct responses: Control: 94,3%, UP: 95.8%, DOWN: 97.9%). Analyzing reaction times to target sounds, we found that participants responded slowest during the cognitive control and fastest during DOWN trials (Figure 6E, left panel, main effect *condition*: $F(2,40) = 35.97$, $p < 0.001$, $\eta_p^2 = 0.64$). Evaluating the relationship between single-trial baseline pupil size prior to targets and reaction times to target sounds revealed a significant positive correlation, indicating that smaller pupil size at target onset was associated with faster responses ($r_{rm} = 0.13$, $p < 0.001$, Figure 6F, right panel; for correlations within conditions, see SF 5B).

Finally, comparing task performance variability by means of the standard deviation (SD) of reaction times revealed a significant difference between conditions (main effect *condition:* $F(2,40) = 4.84$, $p = 0.01$, $\eta_p^2 = 0.19$; Figure 6E, right panel) mainly driven by less variable responses in DOWN than control trials.

Our results reveal that self-regulating pupil diameter as a proxy of LC-mediated arousal facilitates adequate behavioral responses as predicted by current theories of noradrenergic function.

Discussion

In a series of experiments, we tested whether participants could gain volitional control over their brain's arousal state via a newly developed pupil-NF approach that we hypothesized to tap into the mechanistic link between LC-NA activity and pupil size. We found that healthy adults can learn to self-regulate pupil size during a 3-days training with veridical pupil-NF but not with sham feedback (Figure 2). Investigating the neural, physiological, and behavioral consequences of up- versus downregulated pupil size revealed three main findings: First, LC activity was significantly modulated during pupil self-regulation together with other arousal-regulating centers, especially the dopaminergic SN/VTA (Figure 3). Second, in line with previous findings showing that the LC exerts a strong influence on the cardiovascular system[8,9,51], we observed systematic changes in cardiovascular parameters, particularly in heart rate (Figure 5). Third, pupil-self-regulation significantly influenced task performance and a well-established psychophysiological readout of phasic LC activity evoked by task-relevant sounds during an oddball task (Figure 6).

Previous research has shown that it is possible to gain volitional control over body and brain functions if bio- or neurofeedback is combined with suitable mental strategies integrated into an appropriate task setting[33,35,36,52]. We showed that providing feedback on pupil diameter significantly enhanced the ability to volitionally up- versus downregulate pupil size when compared (i) within participants from pre- to post-training and (ii) between a veridical and sham neurofeedback group. Interestingly, upregulation was already strong during the first neurofeedback session, while downregulation evolved over the course of training. This is in line with previous reports[30,32], where only upregulating but not downregulating pupil diameter was successful when participants were in a resting state and trained for one session[32]. Our results further suggest that once acquired and optimized, self-regulation of pupil size is a skill that can be controlled in a feedforward manner and is no longer dependent on receiving constant feedback. Even though we tested this ability in a no-feedback-phase immediately after training, previous studies showed lasting self-regulation of central nervous system activity providing evidence that it is possible to retain this skill over time[33].

We had hypothesized that volitional pupil size modulation is linked to activity changes in brain nuclei regulating the brain's arousal levels and in the LC in particular. Intriguingly, our ROI analysis on brainstem fMRI data during pupil self-regulation confirmed this hypothesis and revealed that up- versus downregulation of pupil size was indeed associated with systematic LC BOLD activity changes. In addition, pupil diameter dynamics throughout a run correlated with LC BOLD activity changes (trend-level effect after correcting for multiple comparisons). Not surprisingly, self-regulating pupil diameter did not exclusively modulate LC activity but led to analogous BOLD activity changes in the

SN/VTA and – less consistently – in the NBM (trends after correction for multiple comparison). These results are in line with a recent study in humans that specifically linked noradrenergic, cholinergic, and dopaminergic activity to pupil responses during a cognitive task[20] and the close interactions between the LC, the basal forebrain including the NBM, and the VTA that have been demonstrated in animal models[53–57]. More specifically, studies in non-human primates and rodents revealed that noradrenergic fibers originating from the LC have a neuromodulatory effect on the VTA and that each LC innervates VTAs in both hemispheres to a similar extent[56,57]. Similarly, in rodents the SN receives NA-projections from the LC[56] suggesting that LC activation may not only have modulatory influences on the VTA but also on the SN. Based on our methodology, however, we cannot reliably disentangle whether SN/VTA modulation during pupil self-regulation is directly achieved via top-down control mechanisms or indirectly via the LC.

Here, links between self-regulating pupil size and the cholinergic NBM only reached trend-level significance and were less consistent than for dopaminergic and noradrenergic regions. A direct comparison of cholinergic and noradrenergic systems and their role in pupil dynamics in mice provided correlative evidence for the involvement of both systems. However, only longer-lasting dilations of the pupil, such as during locomotion, were accompanied by sustained cholinergic activity, while moment-to-moment pupil fluctuations during rest closely tracked noradrenergic activity[21]. Furthermore, noradrenergic activity preceded cholinergic activity relative to peak pupil dilation[21], which, together with the finding that noradrenergic neurons can depolarize cholinergic neurons[1], has led to the assumption that noradrenergic activity may drive cholinergic activation. However, even the limited temporal resolution of fMRI measures does not allow us to reliably test this proposal in our human dataset.

Self-regulating pupil diameter, did not systematically modulate BOLD responses in the DRN and SC in our ROI analyses, two brainstem regions that have been implicated in non-luminance-dependent pupil size changes[19,40]. The absence of an effect in the SC is in line with the theory that it modulates pupil mainly in the context of specific orienting responses towards salient events while LC modulates pupil in the context of arousal[58,59].

Our explorative general linear model analyses on brainstem fMRI data revealed activation at other critical nodes for producing a waking state and regulating autonomic activity including the pedunculopontine nucleus and the periaqueductal gray (see ST 2AB), emphasizing that self-regulating pupil dynamics may modulate a distributed brainstem network related to arousal regulation. It is, however, unclear whether these effects are driven directly via cortical and/or subcortical top-down control mechanisms or rather through the LC as a major relay station. To disentangle whether the seemingly synchronized up- and downregulation of different neuromodulatory systems and brainstem

nuclei during pupil self-regulation is orchestrated indirectly via the LC, future research could combine pupil-NF with pharmacological agents targeting different systems.

It is important to stress that imaging the human brainstem, and the LC in particular, is extremely challenging due to the small nuclei, high susceptibility to physiological noise, and lower signal-to-noise ratio than cortical signals. Here, we report exploratory, data-driven brainstem analyses at uncorrected levels[28]. However, we are confident that our findings represent reliable results because we applied stringent noise control by means of independent component analysis (ICA) and physiological noise modeling (PNM). Given the correlation between heart rate and pupil self-regulation, considering heart rate as a nuisance regressor during PNM may have additionally weakened our results and may provide a rather conservative perspective. Furthermore, our exploratory, data-driven fMRI analyses only complemented ROI analyses corrected for multiple comparisons.

Our study has also identified candidate areas that might exert top-down control of the arousal system in the brainstem. Up- as compared to downregulation of pupil size was associated with BOLD activity changes in brain regions heavily interconnected with the brainstem and with the LC in particular, including the ACC, OFC, DLPFC, the precuneus, thalamus, globus pallidus, and the cerebellum. Our analyses do not allow us to determine whether activity in these areas is causal for arousal modulation or rather its consequence. However, it is tempting to speculate that particularly frontal areas such as the ACC and OFC that have dense projections to the LC in non-human primates[4,60] form the brain's intrinsic control system of arousal and exert top-down control of LC activity.

Together, our fMRI results show that pupil size not only can be used as an indirect readout for arousal[20,22,23], but also provides an active information channel for self-regulating activity in areas involved in arousal regulation. Our results implicate the LC as an important brainstem area that is significantly modulated by pupil self-regulation which, in turn, might modulate activity in other downstream areas involved in arousal control.

Pupil dilation responses evoked by an oddball task have been suggested to represent a psychophysiological marker of phasic LC activity[4,61,62]. Additionally, well-known theories derived from work in animal models postulate that phasic LC activity in response to task-relevant events depends on tonic LC activity: when tonic LC activity is upregulated, phasic LC responses are weak; whereas when tonic LC activity is relatively lower, phasic LC responses are strong[4,18]. A similar relationship has been observed in human pupil measurements reporting an inverse relationship between naturally fluctuating baseline pupil size and pupil dilation responses[61–63]. In line with these previous results, we found that downregulating pupil diameter in a sustained way at baseline, led to larger pupil dilation responses and faster and more consistent reaction times to target sounds. By contrast, upregulating pupil diameter at baseline led to smaller pupil dilation responses and longer reaction times. These results are consistent with previous work, strongly suggesting that self-regulating

pupil diameter modulates tonic LC activity. Our behavioral findings further confirm previous studies reporting enhanced task performance with a relatively low baseline pupil diameter, either when changes in baseline diameter are experimentally induced[64] or occur spontaneously[61] (however, see[62]) whereas high baseline pupil size, assumed to reflect high tonic activity, might be detrimental to task engagement and performance[15,17]. Taken together, our data supports the idea that the state of tonic LC activity reflected by baseline pupil size prior to target onset predicts the pupil dilation response, a peripheral marker of phasic LC responses, and attentional performance. Such an influence may be achieved via a modulation of ongoing processes in cortical target areas of NA projections facilitating adequate behavioral responses.

In our oddball task, we also implemented a control condition where participants had to count backwards in steps of seven while responding to target tones. To our surprise, absolute pupil size was substantially higher in this condition already at baseline. This suggests that our counting task was cognitively effortful leading to increased pupil diameter throughout the task. Despite these differences in pupil size, we did not find a significant difference in pupil dilation responses to target sounds between the control and downregulation conditions. Furthermore, participants showed the slowest and most variable responses to task-relevant sounds in control trials. We can only speculate that these effects may have been due to high cognitive load resulting in dual task costs of counting and responding to target sounds at the same time. These costs may have been reduced for self-regulation trials since participants had been practicing this skill over several days resulting in more automatized processes.

Since the LC plays a central role in controlling autonomic activity through projections to structures involved in cardiovascular regulation[8,9,51], we investigated whether self-regulating pupil diameter affects cardiovascular parameters. In line with our hypothesis, we observed that heart rate was generally higher for up- versus downregulation of pupil size, an effect that increased from session to session and was related to the ability to self-regulate pupil size following pupil-NF training. The effects on HRV indicated by RMSSD values were less clear. Only during fMRI sessions, we found a trend towards higher RMSSD during down- than upregulation which may potentially indicate increased parasympathetic activity during down- relative to upregulation trials[65]. One must keep in mind, that our pupil-self regulation period was only 15s. Given this rather short modulation period, our strong effects in heart rate and trend-level effects in HRV are quite a remarkable finding. Applying pupil-self regulation for longer periods will allow us to investigate whether this new intervention can modulate heart rate and potentially also HRV over longer time scales, supposedly via the LC-NA system that acts on structures involved in autonomic and cardiovascular regulation.

In summary, we provide evidence that our pupil-NF approach allows healthy volunteers to gain volitional control of their pupil size. Self-regulation of pupil size is associated with systematic

modulation of activity in several brainstem nuclei that control the brain's arousal state, including the LC and SN/VTA. We could further show that self-regulation of pupil size modulates (i) cardiovascular parameters and (ii) psychophysiological and behavioral outcomes measured during an oddball task closely linked to LC activity. Thus, even though pupil-based self-regulation modulates various areas involved in arousal control, our study has revealed convergent evidence suggesting that volitionally controlling pupil size affects LC activity. The introduced pupil-NF approach may constitute a completely novel tool to experimentally modulate arousal-regulating neuromodulatory systems in general and LC activity in particular. Considering the strong modulatory effects of the LC-NA system on cognitive function and various behaviors including stress-related responses, pupil-NF has enormous potential to be translated to behavioral and clinical applications across various domains.

Methods

General information

All participants included in the studies were healthy adults, free of medication acting on the central nervous system, with no neurological and psychiatric disorders and with normal or corrected-to-normal vision by contact lenses. All participants were asked to abstain from caffeine intake on the day of testing. All experimental protocols were approved by the research ethics committee of the canton of Zurich (KEK-ZH 2018-01078) and conducted in accordance with the declaration of Helsinki. All participants provided written informed consent prior to study participation and received monetary compensation.

Experiment 1A: Pupil-NF training to learn to volitionally regulate pupil size

Participants

A priori power analyses based on own pilot data of a single training session with 30 trials (unpublished data) aiming for a power level of 80% resulted in a necessary sample size of 31 participants. As we expected training effects of our multi-session approaches, we recruited 28 participants for the NF (24 ± 5 years, 16 females) and 28 participants for the control group (24 ± 5 years; 13 females) of Experiment 1A, exceeding the sample size of other NF studies[33,66,67]. Participants were randomly assigned to the pupil-NF or control group. Developing an eye blink-related strategy instead of a mental strategy (one pupil-NF participant) and a drop-out after the first session due to personal reasons (one control participant) led to a final sample size of n = 27 for the pupil-NF group and n = 27 participants for the control group, respectively.

Pupil-based neurofeedback

Participants sat in a comfortable chair with their chin placed in a chinrest to ensure a stable head position without putting too much strain on the neck of the participants. We kept the height of the chin rest constant across participants and adjusted the height of the chair to accommodate participants[68]. Their eyes were ~65cm away from the eye tracker (Tobii TX300, Tobii Technology AG, Stockholm, Sweden) that was positioned below the screen (240B7QPJ, resolution: 1680x1050; Philips, Amsterdam, Netherlands) to allow for optimal eye tracking and measurement of pupil size. They were instructed to look at the fixation dot displayed in the center of the screen. Pupil diameter and eye gaze data of both eyes were sampled at 60 Hz. To ensure that participants did not use eye movement-related strategies (e.g., vergence movements, squinting), we additionally videorecorded the right eye of the participants and visually inspected these videos. At the start of each session, the eye tracker was calibrated using a 5-point calibration.

In all three training sessions, participants received online (quasi real-time) and post-trial feedback on their pupil modulation performance that was based on estimating pupil size of the dominant eye. We accounted for artifacts caused by eye blinks, physiological and measurement-based noise with the following preprocessing steps: (i) rejection of data samples containing physiologically implausible pupil diameter values ranging outside of a pupil size of 1.5 and 9mm – this step also ensured that blinks, recorded with a value of -1, would not be included in feedback shown to participants; (ii) rejection of physiologically implausible pupil size changes larger than 0.0027mm/s. This previously implemented approach[32,69] is based on specifications of a study reporting peak velocity of the pupillary light reflex[70]. Finally, to ensure a smooth feedback display, the last two collected and processed pupil size samples were averaged and displayed[32]. During the pupil self-regulation phase, pupil size was displayed on the screen by means of a moving circle (Figure 1C, upper panel) centered around the fixation dot. This moving circle showed pupil size relative to a dashed circle representing the mean pupil size of a 5s baseline phase (i.e., when participants did not self-regulate pupil size). Importantly, the moving circle only indicated pupil size changes in the required direction, e.g., getting larger for upregulation and smaller for downregulation trials. If pupil size didn't change in the required direction, the circle stayed at the size of the baseline circle. The thickness of the circle was adjusted relative to its size so that the numbers of pixels shown on the screen were kept constant throughout the modulation phase. After completion of the modulation phase, post-trial performance feedback was displayed. Here, valid pupil diameter samples were averaged across the modulation phase, the maximum change was extracted and displayed on the screen with average feedback being color-coded: If participants successfully modulated pupil size into the required direction (i.e., pupil size during modulation was larger than baseline pupil size in upregulation trials or smaller than baseline pupil size in downregulation trials), the circle indicating the average change was shown in green (Figure 1C). If pupil size modulation was not successful (i.e., pupil size during modulation was similar to or smaller

than the baseline pupil size in the upregulation trials or bigger than baseline pupil size in downregulation trials), the circle was depicted in red. The maximum change was always indicated in black. This intermittent feedback was displayed for 2s.

Throughout the experiment, we ensured that all colors were isoluminant to the grey background (RGB [150 150 150]) by calculating relative luminance as a linear combination of red, green, and blue components based on the formula: $Y = 0.2126\ R + 0.7152\ G + 0.0722\ B$. It follows the idea that blue light contributes the least to perceived luminance while green light contributes the most (https://www.w3.org/Graphics/Color/sRGB). Stimulus presentation throughout the experiment was controlled using the MATLAB-based presentation software Psychtoolbox 3.0.17.

All participants underwent three sessions of pupil-NF on separate days within a period of seven days. The pupil-NF training session took place roughly at the same time of the day to keep circadian influences constant. Prior to pupil-NF training on day 1, participants read an instruction sheet explaining the procedures and providing recommended mental strategies derived from previous publications of dilated or constricted pupil size during different mental states and cognitive or emotional tasks[29,32,37–39]. Participants were informed to rely on these (or similar) mental strategies. Furthermore, we determined the dominant eye of each participant (right eye dominance: n = 22 pupil-NF group; n = 20 control group) since the displayed feedback during training was determined by the data recorded of the dominant eye using the Miles test[71].

In each of the training sessions, three up- and three downregulation blocks were performed, each consisting of ten trials (30 UP/30 DOWN trials per day; Figure 1B). Each trial (Figure 1C) started with the display of the direction of modulation (either up- or downregulation) in green for 2s on a grey background followed by a baseline phase of 7s. Participants saw a green fixation dot in the center of a screen surrounded by a dashed green circle during baseline. During this baseline phase, participants were instructed to silently count backwards in their heads in steps of four to bring them into a controlled mental state. Then, a 15s modulation phase indicated by the display of an additional solid green circle started in which participants were asked to use mental strategies to up- or downregulate their own pupil size while receiving online pupil-NF. This modulation phase was followed by post-trial performance feedback for 2s. After a break of 5s indicated by the words “short break” in green, a new trial started. After each block, participants could take a short self-determined break before they continued with the next block.

On training day 3, participants performed additional no-feedback-trials following the same overall structure. However, the start of the modulation phase was indicated by a change from an “=” to an “x” in the same color (green) and same position above the fixation dot. No baseline circle was shown and no feedback, neither online nor post-trial performance feedback was provided.

After the pupil-NF sessions, we conducted a debriefing in which participants reported in their own words which mental strategies they used for up- and downregulation, respectively.

Training sessions of the control group

Participants of the control group experienced identical conditions as participants of the pupil-NF group including the same instructions on mental strategies for up- and downregulations and the same amount of training. However, veridical feedback was not provided. To ensure a similar visual input as for the NF group, each participant of the control group saw a version of the visual input from one participant of the NF group resulting in the same proportion of positive/negative performance feedback as in the NF group. However, to prevent the development of illusory correlations, participants were informed that this will occur at a fixed rate. As in the pupil NF group, control participants were instructed to look at the fixation dot in the center of the screen and to focus on the mental strategies introduced to them.

Offline data processing and analysis of pupil data

(Pre-)processing of the pupil data was conducted using Matlab R2018a (MathWorks, Inc., Natick, MA, USA). Recorded pupil size (in mm), gaze data, and video recordings were visually inspected to ensure that participants followed the instructions to look at the fixation dot in the center of the screen during the baseline and modulation phase of the experiment and did not use eye movement related strategies (e.g., vergence movements or squinting). In case of violations during these phases (i.e., squinting/opening eyes systematically, large eye movements/saccades, i.e., deviations > ~16° and ~10° of visual angle on the x- and y-axes, respectively) that can potentially bias the validity of measured pupil size[68], trials were excluded from further analysis (pupil-NF group = 8.5%; control group = 7.4%; $t(52) = -0.8$; $p > 0.42$). Then, pupil data of both eyes were systematically preprocessed using the guidelines and standardized open source pipeline published by Kret and Sjak-Shie[72]. Invalid pupil diameter samples representing dilation speed outliers and large deviation from trend line pupil size (repeated four times in a multipass approach) were removed using a median absolute deviation (MAD; multiplier in preprocessing set to 12[72]) – a robust and outlier resilient data dispersion metric. Further, temporally isolated samples with a maximum width of 50ms that border a gap larger than 40ms were removed. Then, we generated mean pupil size time series from the two eyes which were used for all further analyses reported (see[72] on how mean times series can be calculated even with sparsely missing samples of one pupil). The data were resampled with interpolation to 1000Hz and smoothed using a zero-phase low-pass filter with a recommended cutoff frequency of four[72]. In a next step, the resulting data were inspected and trials with more than 30% of missing data points across baseline and modulation phases were excluded. Sessions with more than 50% of missing trials of a participant were excluded from further analysis (n = 1 in the pupil-NF group: participant who

developed the eye blink-related strategy). Finally, preprocessed pupil diameter was corrected relative to baseline, by computing mean pupil size of the last 1000ms before the start of the modulation phase of each trial and subtracting this value from each sample of the respective modulation phase, as previously recommended[73].

In a next step, we averaged the baseline-corrected pupil diameter time series during baseline and modulation phases across the UP and DOWN condition of each session (day 1, day 2, day 3, no feedback post) and participant. Furthermore, for each participant and each session, absolute baseline diameter used for trial-based baseline correction (i.e., averaged across 1000ms before modulation onset) was calculated for each condition (i.e., UP and DOWN). To determine whether it is possible to learn to volitionally modulate pupil size, and to determine whether veridical pupil-NF is essential for successful self-regulation, we calculated a pupil modulation index for all participants of both groups for each session (day 1, day 2, day 3, no feedback post) by subtracting baseline-corrected pupil changes averaged across the 15s modulation phase during DOWN from baseline-corrected pupil changes averages across the 15s modulation phase during UP (i.e., UP – DOWN). Larger modulation indices indicate better condition-specific modulation.

Statistical analyses were performed using IBM SPSS 28 (IBM Corporation, Armonk, NY, USA), R version 4.1.2 (R Core Team), and JASP (version 0.16.2; https://jasp-stats.org/). Since Shapiro-Wilk tests revealed significant deviations from Gaussian distribution of some of the residuals of the pupil modulation index (UP – DOWN) for both groups, we computed robust mixed design ANOVAs based on 20% trimmed means using the R package WRS2 (version 1.1-3; https://cran.r-project.org/web/packages/WRS2/index.html) to compare the pupil modulation indices with the within-subjects factor *session* (day 1 versus day 2 versus day 3 versus no feedback post) and the between-subjects factor *group* (NF versus control). In case of significant effects, we derived post-hoc *p*-values using bootstrap-based functions implemented in the WRS2 package. Finally, we performed statistical analyses to ensure stable pupil size during baseline phases. To this end, we subjected absolute baseline pupil size averaged for each session and condition across participants of each group to a mixed design ANOVA with the within-subjects factors *session* (day 1 versus day 2 versus day 3 versus no feedback post) and *condition* (UP versus DOWN) and the between-subjects factor *group* (pupil-NF versus control). Sphericity was assessed using Mauchly's sphericity test and violations were accounted for with the Greenhouse-Geisser correction. In case of significant effects, we derived post-hoc *p*-values corrected for multiple comparisons using sequential Bonferroni correction[41]. Additionally, we ran a Bayesian ANOVA using the same factors to be able to evaluate whether there is evidence for the null hypothesis (i.e., no difference in baseline pupil size between conditions in neither session nor group) and default priors.

Experiment 1B: Replication of Experiment 1A

Participants

We recruited an independent cohort of 26 participants (18 females, 26 ± 7 years). Technical issues with the eye tracker led to an interruption of training and exclusion of one participant (n = 25 for final analyses).

Pupil-based neurofeedback

The paradigm used was identical to Experiment 1A with two implemented changes: (i) we added a no feedback session *prior* to training (Pre) in which participants only used instructed mental strategies without receiving any feedback; (ii) online feedback on training day 3 was removed and participants only received post-trial performance feedback (SF 2A). As during no feedback trials, the baseline phase was indicated by a "=" above the fixation dot on the screen, changing to an "x" as soon as the modulation phase started. Trial timing and instructions remained the same as in Experiment 1A**.**

Cardiovascular measurements

For 15 participants (11 females, 25 ± 6 years), we additionally recorded cardiac data with a Biopac MP 160 system and the accompanying AcqKnowledge software (Biopac Systems Inc., USA). ECG was recorded continuously and sampled at 1000Hz from two electrodes, one attached to the left lower rib and one under the right collarbone. An electrode attached to the left collarbone was used as a reference. All physiological data was recorded and stored on a PC for off-line analysis. We also recorded continuous respiration data by means of a breathing belt (Biopac Systems Inc., USA) that was affixed to the participant's chest, however, respiratory data is not reported here.

Pupil data (pre-)processing and analysis

The no feedback session (Pre and Post pupil-NF training) allowed us to directly compare self-modulation performance without feedback effects in the same group of participants. We excluded 5.4% of all trials due to violations during baseline and modulation phases (i.e., squinting/opening of the eye in a systematic way, large eye movements/saccades). Baseline-corrected pupil size time series during self-regulation were calculated as described in Experiment 1A. We statistically compared these time series Pre and Post pupil-NF training by subjecting the data to a two-way repeated measures ANOVA with the within-subjects factors *condition* (UP versus DOWN) and *session* (Pre versus Post pupil-NF training) using the MATLAB-based SPM1D toolbox for one-dimensional data (SPM1D M.0.4.8;

https://spm1d.org/). SPM1D uses random field theory to make statistical inferences at the continuum level regarding sets of one-dimensional measurements. It is based on the idea to quantify the probability that smooth, random one-dimensional continua would produce a test statistic continuum whose maximum exceeds a particular test statistic value and has been previously used to analyze one-dimensional kinematic, biomechanical or force trajectories[74,75]. In case of significant effects, post-hoc tests implemented in the SPM1D software were used which are corrected for multiple comparisons using Bonferroni corrections.

Cardiac data (pre-)processing and analyses

ECG R peaks were detected automatically and, if necessary, manually corrected using the MATLAB-based toolbox PhysioZoo[76]. Data segments consisting of non-detectable peaks or poor quality were excluded from further analyses. Resulting R-R intervals for which both R peaks were occurring in the modulation phase of the pupil-NF training were extracted and further processed in MATLAB (R2021a). Data of one participant was disrupted and excluded since it was not possible to detect R peaks for no feedback trials prior to training. Missing data was replaced by the group mean so as not to further reduce statistical power. Heart rate, reflecting cardiovascular dynamics controlled by an interplay between the sympathetic and parasympathetic nervous system, was calculated by dividing 60 through the respective R-R intervals of the modulation phase. Furthermore, we computed the RMSSD calculated based on R-R-intervals. We chose RMSSD because it is relatively free from breathing influences[77] and can be computed for intervals as short as 10s[78,79]. It represents a beat-to-beat measure of HRV in the time domain that is assumed to give meaningful insights about parasympathetic activity of the autonomic nervous system. Heart rate and RMSSD calculated for each modulation phase was averaged across the respective up- and downregulation condition of each training session.

To investigate whether pupil self-regulation systematically modulates cardiovascular parameters, we subjected heart rate averages for each condition (UP versus DOWN) and training session (no feedback pre, day 1, day 2, day 3, no feedback post) to a two-way repeated measures ANOVA. Sphericity was assessed using Mauchly's sphericity test and violations were accounted for with the Greenhouse-Geisser correction. Since our HRV measure, RMSSD, significantly deviated from normal distribution (Shapiro-Wilk tests, all $p < 0.01$), we calculated differences scores in RMSSD between up- and downregulation trials (DOWN-UP) for each session (no feedback pre, day 1, day 2, day 3, no feedback post). Positive values indicated larger HRV in DOWN than UP trials and negative values indicated larger HRV in UP than DOWN trials. These difference scores were subjected to a robust ANOVA using the WRS2 package of R. In case our analyses yielded significant effects, post-hoc tests were conducted. To determine whether potential differences in cardiac dynamics between UP and DOWN trials were associated with volitional pupil modulation performance prior to training, we calculated

Spearman correlation coefficients between the pupil modulation index (i.e., UP–DOWN) and heart rate (UP–DOWN) or RMSSD (DOWN–UP). Reported statistical analyses were two-tailed tests and corrected for multiple comparisons using sequential Bonferroni correction[41] or Hochberg's approach implemented in the WRS2 package of R.

Experiment 2: Pupil-NF combined with simultaneous fMRI

Participants

For Experiment 2, we re-recruited 25 participants (17 females; age 25 ± 5 years) from the pupil-NF groups of Experiments 1A and B, a sample size that is bigger or comparable to those in previous fMRI studies showing significant correlations between pupil measures and brain activity[20,22,23]. Additional exclusion criteria were: (i) metal implants and/or fragments in the body, (ii) suffering from claustrophobia, and (iii) pregnancy at the time of the experiment. In case the last session of pupil-NF took place more than ten days before the scheduled fMRI session, participants received one session of re-training combining 40 trials of online feedback (i.e., 20 trials UP and DOWN, respectively) and 20 trials of only post-trial feedback (i.e., 10 trials UP and DOWN, respectively) in the week before the first fMRI session. This re-training was included to assure that participants were still able to modulate their own pupil size successfully. Re-training data is not reported here.

Data acquisition

All volunteers participated in two fMRI sessions, one using an optimized brainstem imaging sequence, the other acquiring whole-brain data (order of sessions was counterbalanced across volunteers). (f)MRI data was acquired on a 3T Philips Ingenia system using a 32-channel head coil. Anatomical images of the brain used for anatomical co-registration were acquired using a T1-weighted sequence (MPRAGE; 160 sagittal slices, TR/TE = 9.3/4.4 ms, voxel size = 0.7 mm^3, matrix size = 240 x 240, flip angle = 8°, FOV = 240 mm (AP) x 240 mm (RL) x 160 mm (FH)). A turbo spin echo (TSE) neuromelanin-sensitive structural scan was acquired for delineation of the LC (not reported here) which was oriented perpendicular to the floor of the fourth ventricle (20 slices, 1.5mm, no gaps, in-plane resolution: 0.7 x 0.88 mm (reconstructed at: 0.35 x 0.35 mm), TR = 500 ms, TE = 10 ms, flip angle = 90˚, covering the brainstem only). During the brainstem session, echo-planar imaging (EPI) scans were acquired in 39 sagittal slices (thickness: 1.8 mm, no gaps) aligned parallel to the floor of the fourth ventricle along the brainstem with the following parameters: TR = 2.5 s, TE = 26 ms, flip angle = 82°, SENSE acceleration factor = 2.1, in-plane resolution of 1.8 x 1.8 mm, and 240 volumes per run. Additionally, a whole-brain single volume EPI image was acquired to improve co-registration between fMRI data and the anatomical MRI scans (identical sequence parameters to the brainstem fMRI sequence).

During the whole-brain session, EPI images were acquired in 40 slices (thickness: 2.7 mm) with the following parameters: TR = 2.5 s, TE = 30 ms, flip angle = 85°, FOV = 223 mm (AP) x 223 mm (RL) x 116 mm (FH), Sense factor 2. Images were acquired at an in-plane resolution of 2.7 x 2.7 mm and were reconstructed at a resolution of 1.74 x 1.74 mm. In each session, we acquired 240 volumes per run. For the first seven subjects, we used an EPI sequence with slightly different details (i.e., especially higher spatial resolution to be able to see brainstem activity in small nuclei; non-isometric: 36 slices (thickness: 3mm, no gaps, TR = 2.5, TE = 30, flip angle 82°, FOV = 210 mm (AP) x 210 mm (RL) x 108 mm (FH), Sense factor 2.2, in plane resolution of 2 x 2 mm reconstructed at a resolution of 1.64 x 1.64 mm), however, due to the strong distortion observed in one excluded participant, we decided to adjust the sequence.

During both MRI sessions, cardiac cycle and respiratory activity were recorded with a sampling rate of 496 Hz with a pulse oximeter attached to the left index finger and a chest belt, respectively (Invivo; Phillips Medical Systems, Orlando, Florida). These data were used for physiological noise removal as well as for calculating cardiovascular parameters.

Concurrently with fMRI recordings, participants' eye gaze and pupil size of the left eye were tracked at 1000Hz using an EyeLink 1000 Plus Long Range Mount (SR Research, Ottawa, Ontario, Canada) that was placed at the end of the scanner bore on an aluminum stand and a first-surface mirror attached to the head coil. At the beginning of each fMRI run, the eye tracker was calibrated using 5-point calibration implemented in the software of the device. Pupil diameter was converted from arbitrary units to mm using the following formula: diameter (mm) = diameter (a.u.) / 1372. The conversion factor was estimated as described in [68,80].

fMRI Paradigm

The pupil-NF paradigm during fMRI was similar to our training paradigm. Participants were instructed to maintain gaze on the green fixation dot presented in the center of the screen. Each trial began with a baseline measurement (7.5s) followed by an UP or DOWN phase (15s; without online feedback) during which participants were asked to apply the acquired respective mental strategy. Participants only received post-trial performance feedback (2.5s). After a short break (randomly jittered between 6-9s), the next trial started. Online processing and calculation of the feedback displayed to participants was performed as in Experiment 1A. The conditions were blocked within each of four fMRI runs, that is four trials of upregulation followed by four trials of DOWN (or vice versa). At the beginning of each block, it was indicated on the screen whether this block contains UP or DOWN trials. After each block, a break of 10s was added to allow participants to take short breaks in between. Each of the runs comprised two blocks of each condition, leading to 32 trials per condition. The order of conditions was

counterbalanced across runs. Further, we counterbalanced across participants what conditions they started the respective fMRI session with.

Processing and analysis of pupil data

Pupil data (pre-)processing was conducted as described for Experiment 1A leading to baseline-corrected pupil diameter time series for UP and DOWN trials for each fMRI session. Similar to Experiments 1AB, absolute baseline pupil diameter was compared by means of a repeated measures ANOVA with the within-subjects factor *session* (brainstem versus whole-brain) and *condition* (UP versus DOWN) and Bayesian repeated measures ANOVAs using default priors.

Finally, preprocessed absolute pupil diameter data were downsampled throughout the whole experiment to match the fMRI volume acquisition by averaging all data within a given TR. Missing pupil diameters were linearly interpolated across adjacent epochs resulting in a pupil diameter vector for each fMRI run.

Processing and analysis of cardiac data

Heart (pulse) rate concurrently measured during fMRI was (pre-)processed as described for Experiment 1B resulting in heart rate and RMSSD averages for each condition (UP and DOWN) and session (brainstem and whole-brain). Due to technical issues (whole-brain session of 1 participant), poor data quality (brainstem session of 1 participant), the final n for heart rate and RMSSD analyses was 24 for each fMRI session. Heart rate data was subjected to a repeated measures ANOVA with the within-subjects factor condition (UP versus DOWN) and fMRI session (brainstem vs. whole-brain). Since RMSSD values did significantly deviate from normal distribution (revealed by Shapiro-Wilk tests $p < .05$), we compared UP and DOWN trials for each fMRI session by means of a Wilcoxon signed rank test implemented in SPSS. Finally, as for the no feedback session prior to pupil-NF training, we calculated Spearman correlation coefficients between the pupil modulation index (UP–DOWN) and differences in heart rate (UP–DOWN) or RMSSD (DOWN–UP) following training during fMRI (averaged across the two sessions). All statistical analyses were computed using SPSS and corrected for multiple comparison using sequential Bonferroni correction.

MRI analysis

MRI data was analyzed using tools from FSL version 6.0 (http://fsl.fmrib. ox.ac.uk/fsl), MATLAB R2018a, and FreeSurfer version 6.0 (https://surfer.nmr.mgh.harvard.edu/).

Pre-processing of brainstem data

Since brainstem fMRI signal is highly susceptible to corruption from physiological sources of noise, we used a rigorous pre-processing pipeline implementing suggestions from previously published research[20,28,81] including the following steps: brain extraction using FSL's automated brain extraction tool (BET;[82]), motion correction using the Linear Image Registration Tool (MCFLIRT;[83]), spatial smoothing using a 3mm full width-at-half-maximum (FWHM) Gaussian kernel, and a 90s high-pass temporal filter as implemented via FSL's Expert Analysis Tool (FEAT;[84]). Additionally, each functional run showing excessive motion with an absolute mean displacement greater than 1 mm (i.e., ~half a voxel size) was excluded (3 runs for 1 participant which led to exclusion from further analyses). To further de-noise the data, we performed Independent Component Analysis (ICA) and FLS's Physiological Noise Modelling (PNM;[85]), an extended version of RETROICOR[86]). ICA denoising was performed using FSL's Multivariate Exploratory Linear Optimized Decomposition Interface (MELODIC,[87]), which allows for decomposition of the fMRI data into spatial and temporal components. The resulting components were visually inspected and classified as "Noise" or "Signal" by two independent researchers using published guidelines[88]. Once labelled, the temporal information of the noise components was extracted and ICA noise regressor lists were generated for later implementation in our general linear model (GLM). For PNM, cardiac and respiratory phases were assigned to each volume in the concatenated EPI image time series separately for each slice. Our complete physiological noise regression model included 34 regressors: 4th order harmonics to capture the cardiac cycle, 4th order harmonics to capture the respiratory cycle, 2nd order harmonics to capture the interaction between cardiac and respiratory cycles, 2nd order harmonics to capture the interaction between respiratory and cardiac cycles, one regressor to capture heart rate, and one regressor to capture respiration volume. Subsequently, we visually inspected the waveforms to assure that the peak of each respiratory and cardiac cycle was correctly marked and adjusted if necessary. The resulting voxelwise confound lists were later added to our GLM. Note that physiological data acquisition was corrupted for one participant. Therefore, this data was analyzed without the PNM regressors. Image co-registration from functional to Montreal Neurological Institute (MNI) standard space was performed by (i) aligning the functional images of each run to each subject's whole-brain EPI image, using the Linear Image Registration Tool (FLIRT) employing a mutual information cost function and six degrees of freedom[89]; (ii) registering whole-brain EPIs to structural T1-weighted images, using a mutual information cost function six degrees of freedom, and then optimised using boundary-based registration (BBR;[90]); (iii) co-registering structural images to the MNI152 ($2mm^3$) template via the nonlinear registration tool (FNIRT) using 12 degrees of freedom[91], and applying the resulting warp fields to the functional images. Each co-registration step was visually inspected using Freeview (FreeSurfer) to ensure exact alignment with an emphasis placed on the pons regions surrounding the LC. Unfortunately, 3 out of 25 participants needed to be excluded

from brainstem fMRI analyses due to heavy distortions (including brainstem regions; 1 participant), excessive motion (1 participant, see above), and periods of sleep during the measurement (1 participant).

Pre-processing of whole-brain data

We used a similar pre-processing pipeline as described above, however, with the following differences: Spatial smoothing was applied using a 5mm full width-at-half-maximum (FWHM) Gaussian kernel. Functional EPI-images were aligned to structural T1-weighted images using linear registration (FLIRT). Structural images were aligned to the MNI standard space using nonlinear registration (FNIRT), and the resulting warp fields applied to the functional images. Data from 1 out of 25 participants showed very strong distortions in temporal and frontal regions and was excluded from further analysis. Also, we needed to exclude 1 functional run for 3 participants and 2 functional runs for 1 participant due to excessive motion with an absolute mean displacement greater than half a voxel size (i.e., 1.4 mm). We did not apply PNM to the data and, as recommended by FSL (https://fsl.fmrib.ox.ac.uk/fsl/fslwiki/FEAT/UserGuide), ICA was only performed (n = 9) if residual effects of motion were still left in the data even after using MCFLIRT for motion correction.

fMRI analyses

Time-series statistical analysis were performed using FEAT with FMRIB's Improved Linear Model (FILM). Two equivalent GLMs were estimated for each session (i.e., for the whole-brain session and the brainstem session).

First, we directly contrasted brain activity during up- versus downregulation periods during whole-brain scans. Therefore, "UP" and "DOWN", were modelled as main regressors of interest for the complete modulation phase of 15s. Instruction, baseline, and post-trial performance feedback periods were modelled as separate regressors. All regressors were convolved with a double gamma HRF and its first temporal derivative. White matter (WM) and cerebrospinal fluid (CSF) time-series, motion parameters and ICA noise component time-series (if applied), respectively, were added as nuisance regressors. Second, we investigated which brain areas would change their activity in close association with pupil diameter. Therefore, pupil diameter was entered as a regressor of interest, together with the same nuisance regressors as described above.

For the brainstem session, we defined GLMs with identical regressors that were, however, convolved with the default optimal basis sets (i.e., the canonical hemodynamic response function (HRF) and its temporal and dispersion derivatives) using FMRIB's Linear Optimal Basis Sets toolkit[92]. This convolution was chosen to account for the possibility that brainstem BOLD responses such as in the LC are not well-modelled solely by the canonical HRF[93]. However, to avoid overestimating

statistical effects, only the canonical HRF regression parameter estimates were used for subsequent higher-level analyses. Additionally, the PNM voxelwise confound lists and the time series of ICA noise components lists were used as nuisance regressors.

All described GLMs were computed separately for each run of each participant and then averaged across runs for each participant in second level analyses using FMRIB's Local Analysis of Fixed Effects[94]. To determine significant effects at the group level, a third level mixed-effects analyses was performed. Group Z-statistic images were thresholded at $Z > 3.1$ for whole-brain analyses and family-wise-error corrected (FWE) at the cluster level. In line with a previous publication[28], we report results for the brainstem analysis at an uncorrected $p < 0.05$, taking into account the limited signal-to-noise ratio for brainstem responses and the small size of the LC in combination with our strict pre-processing pipeline. Here, we implemented a minimum cluster size of 10 voxels, derived from the smallest mask of a recently published brainstem atlas covering all important brainstem nuclei involved in arousal and motor control[42–48]. To visualize brainstem activity, we created a mask covering the brainstem (derived from the Harvard-Oxford subcortical atlas; thresholded at 0.5 and binarized using FSL's image calculator fslmaths) and the NBM (Ch4 cell group derived from the JuBrain/SPM Anatomy Toolbox[49]), showing Z-statistic images within these predefined regions.

Regions of Interest (ROI) analysis

We conducted a series of ROI analyses, to test our hypothesis that self-regulation of pupil size is linked to activity changes in the LC and other neuromodulatory, arousal-regulating centres in the brain. Our principal region of interest was (i) the LC, however, given the close interaction with other brainstem areas and neuromodulatory systems involved in pupil control, we defined secondary ROIs, namely (ii) the cholinergic NBM, (ii) the dopaminergic SN/VTA, (iii) the serotonergic DRN, and (iv) the SC – a specialized motor nucleus in the midbrain implicated in the pupil orientation response – as a control region. Probabilistic anatomical atlases were used to define the location of the brainstem ROIs[42–48] and the NBM (Ch4 cell group[49]; see Figure 3F) in MNI space. After careful visual inspection, we decided to threshold the SC and DRN mask at 0.1, and the SN/VTA-mask at 0.3. The masks for all ROIs were binarized. In a next step, we extracted the average mean signal intensity (Z-values) within each ROI from the second-level fixed effects analysis conducted for each participant for each GLM (i.e., for UP versus rest and DOWN versus rest, and pupil diameter vector used as regressor). Due to deviation from normal distribution for the NBM (Shapiro-Wilk tests; $p < .05$), we used Wilcoxon signed rank tests to test for a significant difference between Z-values for UP and DOWN periods within each ROI, as well as for a significant correlation between absolute pupil diameter and BOLD activity within each ROI (i.e., deviating from 0). All analyses were two-tailed tests corrected for multiple comparisons using sequential Bonferroni correction.

Experiment 3: Pupil-NF combined with an auditory oddball task

Participants

Experiment 3 involved 22 participants (15 females; 26 ± 6 years) of the 25 participants re-recruited for the fMRI experiment. Unfortunately, 3 participants dropped out because of personal reasons. Participants received one session of re-training combining 40 trials of online feedback (i.e., 20 trials UP and DOWN, respectively) and 20 trials of post-trial feedback (i.e., 10 trials UP and 10 DOWN, respectively) within 7 days prior to Experiment 3, in case the last session of pupil-NF took place more than ten days before the scheduled pupil-NF oddball session. This re-training was included to assure that participants were able to modulate their own pupil size successfully. Re-training data is not reported here.

Paradigm: Pupil-NF with an integrated auditory oddball task

The auditory oddball task during pupil-NF consisted of 186 target (~20%) and 750 standard (~80%) tones (440 and 660 Hz with the pitch for target being counterbalanced across participants) delivered for 100ms via headphones at approximately 60dB (Panasonic RP-HJE125, Panasonic Marketing Europe GmbH, Wiesbaden, Germany), and was embedded in our pupil-NF paradigm during which participants were volitionally up- or downregulating their own pupil size via acquired mental strategies. In addition to these two self-regulation conditions, we added a third control condition in which participants were asked to count back in steps of seven instead of self-regulating pupil size. To ensure that participants stick to this task, they were occasionally prompted to enter the final number (after every 6th counting trial). This condition was added to control for effort-effects related to pupil self-regulation and to check whether oddball responses differ in self-regulated as compared to more natural fluctuations in pupil size. At the beginning of the task, participants were reminded to focus on their mental strategies and to pay attention to the tones at the same time.

Each pupil-NF-oddball trial began with a short instruction (2s) indicating the required pupil self-regulation direction (i.e., UP or DOWN) or the counting control condition followed by a baseline measurement of 4s in which participants were asked to silently count backwards in steps of seven. Then, participants were asked to apply the acquired mental strategy to up- or downregulate pupil size for 18s or to continue counting (i.e., control). During this self-regulation or counting phase, eight tones (one or two targets and seven or six standards) were played, and participants were asked to respond to targets but not to standards by pressing a key as quickly as possible with the index finger of their preferred hand. The first tone which was always a standard in each self-regulation or counting phase was played after the first jitter phase (1.8 – 2.2s after the baseline phase) to ensure that participants already reached some modulation of pupil size before the first target appeared. The inter-stimulus interval (ISI) between tones was randomly jittered between 1.8 – 2.2s. Between two targets, there were

at least two standards presented leading to a minimum ISI of 5.4s between two targets allowing the target-evoked pupil dilation response to return to baseline between targets. After each trial, participants received post-trial feedback on average and maximum pupil diameter change for 2s. After a short break of 2s, the next trial started. The calculation of feedback was similar to Experiment 1A, except that only the last two seconds of the baseline phase were considered due to the shortened baseline phase of 4s. For counting trials without feedback phases, counting was followed by a 4s break to keep trial timings similar. Instructions and indication of task phases on the screen were displayed as in Experiment 1B on Day 3. However, to improve visibility further, indication of task phase changes from baseline measurements to self-regulation was displayed in magenta (instead of green) isoluminant to the gray background (Figure 6A).

The pupil-NF conditions were blocked, each block containing 13 trials of UP, DOWN, and control, respectively. The number and order of tones was the same for each pupil-NF condition. After each block, participants could take a self-paced break. In total, the task consisted of nine blocks leading to 117 pupil-NF trials in total. The order of blocks was pseudorandomized in the sense that each condition needed to be presented once (or twice) before another condition was presented for the 2nd (or 3rd) time.

Physiological data acquisition

Eye gaze, pupil diameter, cardiac and respiratory data were recorded throughout the task as described in Experiment 1A and B. Additionally, we acquired electroencephalography (EEG) data using 64 Ag/AgCl actiCAP active surface electrodes, an actiCHamp Plus amplifier and the Brain Vision Recorder proprietary software (Brain Products, Munich, Germany). However, cardiac, respiratory and EEG data are not reported here.

Data (pre-)processing and statistical analyses

Pupil-NF: Self-regulation of pupil size under dual task conditions

Pupil data (pre-)processing was conducted as described for Experiment 1A. We had to exclude 2 participants from further analyses leading to a final n = 20 for pupil data analyses: one participant showed a very high blink rate during the oddball with more than 30% of missing samples during baseline and self-regulation or counting phases for more than 50% of the trials. A second participant showed a similar pattern with more than 30% of missing samples in 35% of the trials, mainly in the control condition (only 20% of the trials were usable after pre-processing). Combined with low behavioral performance (correct responses to targets deviated more than 3 SD from the group mean), we decided to exclude this participant from pupil and behavioral data analyses. For each of the remaining participants, we derived *absolute* and *baseline-corrected* pupil diameter time series averaged for UP, DOWN or counting trials throughout the baseline and self-regulation or counting

phases of the pupil-NF oddball task. Both absolute and baseline-corrected pupil diameter time series were extracted since we expected to observe target-evoked pupil dilation responses that depend in size on absolute pupil size prior to tone onset. Baseline correction was applied as described above, choosing a baseline of 1s prior to self-regulation and counting, respectively.

For statistical analyses of self-regulated pupil size, we averaged preprocessed, baseline-corrected pupil diameter time series for each condition across the entire self-regulation or counting phase to test whether participants were able to successfully self-regulate pupil size even under challenging dual-task conditions. Since these data were deviating from normal distribution (Shapiro Wilk test; $p < 0.05$), we subjected the data to a robust repeated measures ANOVA implementing 20% trimmed means with the factor *condition* (UP versus DOWN versus control; R package WRS2). In case of a significant main effect, we computed the corresponding post-hoc tests included in this R package with implemented FWE correction. Next, we averaged absolute pupil diameter samples across the last second of the baseline phase and subjected it to a repeated measures ANOVA with the within-subjects factor *condition* (UP versus DOWN versus control) to compare absolute baseline pupil diameter between the three conditions. Sphericity was assessed using Mauchly's sphericity test and violations were accounted for with the Greenhouse-Geisser correction. In case of a significant effect, post-hoc tests were conducted using the sequential Bonferroni correction for multiple comparisons. In case of no significant effect, we ran an analogous Bayesian repeated measures ANOVA using JASP (with default priors) to evaluate whether there is evidence for the null hypothesis (i.e., no baseline differences between conditions). All reported statistical analyses were two-tailed tests.

Pupillary responses to presented tones during the oddball task: Pre-tone baseline pupil diameter and pupil dilation responses

We extracted 3.5s epochs around each standard or target tone from -0.5 to +3s relative to tone onset. Pre-tone pupil diameter was calculated by averaging 500ms of pupil diameter data preceding tone presentation. The pupil time series was then (i) normalized to this pre-tone pupil diameter baseline and (ii) averaged for each stimulus type (standard versus target) and condition (UP versus DOWN versus control).

To compare *target*-evoked pupil dilation responses between conditions, we subjected the baseline-corrected pupil dilation response time series to targets grand-averaged within each condition to a repeated-measures ANOVA with the within-subjects factor *condition* (UP versus DOWN versus control) using the SPM1D toolbox. This time series data analysis allowed us to compare both peak dilation towards targets and the shape of the dilation response statistically. The same analysis was repeated for pupil dilation responses to standard tones as a control analysis. In case of significant main effects, post-hoc tests implemented in the SPM1D software corrected for multiple comparisons using Bonferroni correction were used.

Behavioral data

Throughout the experiment, we recorded the correctness of responses and reaction times to tones. Responses to standard tones (i.e., false alarms) and responses for which reaction times exceeded two SD below or above the mean of the respective participant were excluded from further reaction time analyses. Lastly, we calculated the percentage of hits (i.e., responses to targets) and false alarms (i.e., responses to standards) and obtained a percentage of correct responses by subtracting these two measures from each other[64].

To investigate whether self-regulation of pupil size modulates behavioral task performance on the oddball task, we subjected individual reaction times to target tones averaged across trials of each condition to a repeated measures ANOVA with the within-subjects factor *condition* (UP versus DOWN versus control). Sphericity was assessed using Mauchly's sphericity test and violations were accounted for with the Greenhouse-Geisser correction. Next, we examined whether not only speed per se but also performance variability indicated by the standard deviation (SD) of reaction times may be modulated by self-regulated pupil size. We subjected the SD of reaction times to a repeated measures ANOVA with the within-subjects factor *condition* (UP versus DOWN versus control). Sphericity was assessed using Mauchly's sphericity test and violations were accounted for with the Greenhouse-Geisser correction. In case of a significant effect, we conducted post-hoc tests controlled for multiple comparisons by means of sequential Bonferroni corrections. Reported statistical analyses were two-tailed tests.

Correlational analyses between pupil and behavioral data

Finally, we computed repeated measures correlation coefficients between the derived single-trial pre-tone absolute baseline pupil diameter (averaged 500ms before target onset), baseline-corrected target-evoked pupil dilation response peaks, and reaction times to targets of all participants using the R package rmcorr[95].

Acknowledgments

The authors would like to express their gratefulness to all participants of the study. We further thank J.W. de Gee for his great help regarding brainstem-specific MRI sequences and V. Zerbi, J. Bohacek, J.M. Shine and O. Harrison for fruitful discussions. S.N.M. discloses support for the research of this work from the Swiss National Science Foundation (SNSF) Spark grant (CRSK-1_190836) and is supported by the Hochschulmedizin Zürich Flagship project STRESS. N.W. is supported by the National Research Foundation, Prime Minister's Office, Singapore under its Campus for Research Excellence and Technological Enterprise (CREATE) programme.

Competing Interests

The authors declare the following competing interests: S.N.M, M.B, and N.W. are co-founders of a company, *MindMetrix* that intends to offer related technology to the consumer market and have a patent application related to used methods pending (patent applicant: ETH Zurich; inventors: M.B, S.N.M, N.W). All other authors declare no competing interests.

References

1 Jones BE. Activity, modulation and role of basal forebrain cholinergic neurons innervating the cerebral cortex. Prog Brain Res 2004; 145:157–69.

2 Jones BE. Arousal Systems. Front Biosci 2003; 8:s438-451.

3 Hasselmo ME, Sarter M. Modes and models of forebrain cholinergic neuromodulation of cognition. Neuropsychopharmacology 2011; 36:52–73.

4 Aston-Jones G, Cohen JD. An integrative theory of locus coeruleus-norepinephrine function: adaptive gain and optimal performance. Annu Rev Neurosci 2005; 28:403–50.

5 Berridge CW. Noradrenergic modulation of arousal. Brain Res Rev 2008; 58:1–17.

6 Samuels ER, Szabadi E. Functional neuroanatomy of the noradrenergic locus coeruleus: its roles in the regulation of arousal and autonomic function part I: principles of functional organisation. Curr Neuropharmacol 2008; 6:235–53.

7 Sara SJ, Bouret S. Orienting and Reorienting: The Locus Coeruleus Mediates Cognition through Arousal. Neuron 2012; 76:130–41.

8 Wood CS, Valentino RJ, Wood SK. Individual differences in the locus coeruleus-norepinephrine system: Relevance to stress-induced cardiovascular vulnerability. Physiol Behav 2017; 172:40–8.

9 Samuels ER, Szabadi E. Functional neuroanatomy of the noradrenergic locus coeruleus: its roles in the regulation of arousal and autonomic function part II: physiological and pharmacological manipulations and pathological alterations of locus coeruleus activity in humans. Curr Neuropharmacol 2008; 6:254–85.

10 Osorio-Forero A, Cardis R, Vantomme G, et al. Noradrenergic circuit control of non-REM sleep substates. Curr Biol 2021; 31:5009-5023.e7.

11 Takahashi K, Kayama Y, Lin JS, et al. Locus coeruleus neuronal activity during the sleep-waking cycle in mice. Neuroscience 2010; 169:1115–26.

12 Kjaerby C, Andersen M, Hauglund N, et al. Memory-enhancing properties of sleep depend on

the oscillatory amplitude of norepinephrine. Nat Neurosci Springer US; 2022; 25:1059–70.

13 Berridge CW, Waterhouse BD. The locus coeruleus-noradrenergic system: modulation of behavioral state and state-dependent cognitive processes. Brain Res Rev 2003; 42:33–84.

14 Eldar E, Cohen JD, Niv Y. The effects of neural gain on attention and learning. Nat Neurosci 2013; 16:1146–53.

15 Aston-Jones G, Rajkowski J, Kubiak P, et al. Locus coeruleus neurons in monkey are selectively activated by attended cues in a vigilance task. J Neurosci 1994; 14:4467–80.

16 Valentino R., Foote S. Corticotropin-Releasing Factor Disrupts Sensory Responses of Brain Noradrenergic Neurons. Neuroendocrinology 1987; 45:28–36.

17 Usher M, Cohen JD, Servan-Schreiber D, et al. The role of locus coeruleus in the regulation of cognitive performance. Science (80-) 1999; 283:549–54.

18 Aston-Jones G, Rajkowski J, Cohen J. Role of locus coeruleus in attention and behavioral flexibility. Biol Psychiatry 1999; 46:1309–20.

19 Cazettes F, Reato D, Morais JP, et al. Phasic Activation of Dorsal Raphe Serotonergic Neurons Increases Pupil Size. Curr Biol 2020; :192–7.

20 de Gee JW, Colizoli O, Kloosterman NA, et al. Dynamic modulation of decision biases by brainstem arousal systems. Elife 2017; 6:e23232.

21 Reimer J, McGinley MJ, Liu Y, et al. Pupil fluctuations track rapid changes in adrenergic and cholinergic activity in cortex. Nat Commun 2016; 7:1–7.

22 Murphy PR, O'Connell RG, O'Sullivan M, et al. Pupil diameter covaries with BOLD activity in human locus coeruleus. Hum Brain Mapp 2014; 35:4140–54.

23 Alnaes D, Sneve MH, Espeseth T, et al. Pupil size signals mental effort deployed during multiple object tracking and predicts brain activity in the dorsal attention network and the locus coeruleus. J Vis 2014; 14:1–20.

24 Joshi S, Li Y, Kalwani RM, et al. Relationships between Pupil Diameter and Neuronal Activity in the Locus Coeruleus, Colliculi, and Cingulate Cortex. Neuron 2016; 89:221–34.

25 Zerbi V, Floriou-Servou A, Markicevic M, et al. Rapid Reconfiguration of the Functional Connectome after Chemogenetic Locus Coeruleus Activation. Neuron 2019; 103:1–17.

26 Megemont M, McBurney-Lin J, Yang H. Pupil diameter is not an accurate realtime readout of locus coeruleus activity. Elife 2022; 11:1–17.

27 Hayat H, Regev N, Matosevich N, et al. Locus coeruleus norepinephrine activity mediates sensory-evoked awakenings from sleep. Sci Adv 2020; 6:eaaz4232.

28 Jacobs HIL, Priovoulos N, Poser BA, et al. Dynamic behavior of the locus coeruleus during

arousal-related memory processing in a multi-modal 7T fMRI paradigm. Elife 2020; 9:1–30.

29 Ekman I, Poikola A, Mäkäräinen M, et al. Voluntary pupil size change as control in eyes only interaction. Proceedings of the 2008 symposium on Eye tracking research & applications 2008. p. 115–8.

30 Ehlers J, Strauch C, Huckauf A. A view to a click: Pupil size changes as input command in eyes-only human-computer interaction. Int J Hum Comput Stud 2018; 119:28–34.

31 Ehlers J, Strauch C, Huckauf A. Training facilitates cognitive control on pupil dilation. Proceedings of the 2018 ACM Symposium on Eye Tracking Research & Applications Association for Computing Machinery (ACM); 2018. p. 1–5.

32 Ehlers J, Strauch C, Georgi J, et al. Pupil Size Changes as an Active Information Channel for Biofeedback Applications. Appl Psychophysiol Biofeedback 2016; 41:331–9.

33 Ruddy K, Balsters J, Mantini D, et al. Neural activity related to volitional regulation of cortical excitability. Elife 2018; 7:e40843.

34 Koush Y, Rosa MJ, Robineau F, et al. Connectivity-based neurofeedback: Dynamic causal modeling for real-time fMRI. Neuroimage 2013; 81:422–30.

35 Lehrer PM, Gevirtz R. Heart rate variability biofeedback: How and why does it work? Front Psychol 2014; 5:1–9.

36 Sitaram R, Ros T, Stoeckel L, et al. Closed-loop brain training: The science of neurofeedback. Nat Rev Neurosci 2017; 18:86–100.

37 Leuchs L, Schneider M, Czisch M, et al. Neural correlates of pupil dilation during human fear learning. Neuroimage 2017; 147:186–97.

38 Partala T, Surakka V. Pupil size variation as an indication of affective processing. Int J Hum Comput Stud 2003; 59:185–98.

39 Franzen PL, Siegle GJ, Buysse DJ. Relationships between affect, vigilance, and sleepiness following sleep deprivation. J Sleep Res 2008; 17:34–41.

40 Joshi S, Gold JI. Pupil size as a window on neural substrates of cognition. Trends Cogn Sci 2020; 24:466–80.

41 Holm S. A Simple Sequentially Rejective Multiple Test Procedure. Scand J Stat 1979; 6:65–70.

42 Bianciardi M. Brainstem Navigator [Tool/Resource.]. Washington: NITRC. https://www.nitrc.org/doi/landing_page.php?table=groups&id=1551. 2021.

43 Bianciardi M, Toschi N, Edlow BL, et al. Toward an In Vivo Neuroimaging Template of Human Brainstem Nuclei of the Ascending Arousal, Autonomic, and Motor Systems. Brain

Connect 2015; 5:597–607.

44 Bianciardi M, Strong C, Toschi N, et al. A probabilistic template of human mesopontine tegmental nuclei from in vivo 7 T MRI. Neuroimage 2018; 170:222–30.

45 García-Gomar MG, Strong C, Toschi N, et al. In vivo probabilistic structural atlas of the inferior and superior colliculi, medial and lateral geniculate nuclei and superior olivary complex in humans based on 7 tesla MRI. Front Genet 2019; 10:1–15.

46 Singh K, Indovina I, Augustinack JC, et al. Probabilistic Template of the Lateral Parabrachial Nucleus, Medial Parabrachial Nucleus, Vestibular Nuclei Complex, and Medullary Viscero-Sensory-Motor Nuclei Complex in Living Humans From 7 Tesla MRI. Front Neurosci 2020; 13:1–11.

47 Singh K, García-Gomar MG, Bianciardi M. Probabilistic Atlas of the Mesencephalic Reticular Formation, Isthmic Reticular Formation, Microcellular Tegmental Nucleus, Ventral Tegmental Area Nucleus Complex, and Caudal-Rostral Linear Raphe Nucleus Complex in Living Humans from 7 Tesla Magnetic Reso. Brain Connect 2021; 11:613–23.

48 García-Gomar MG, Videnovic A, Singh K, et al. Disruption of Brainstem Structural Connectivity in REM Sleep Behavior Disorder Using 7 Tesla Magnetic Resonance Imaging. Mov Disord 2022; 37:847–53.

49 Eickhoff SB, Stephan KE, Mohlberg H, et al. A new SPM toolbox for combining probabilistic cytoarchitectonic maps and functional imaging data. Neuroimage 2005; 25:1325–35.

50 Rajkowski J, Kubiak P, Aston-Jones G. Locus coeruleus activity in monkey: Phasic and tonic changes are associated with altered vigilance. Brain Res Bull 1994; 35:607–16.

51 Li DP, Atnip LM, Chen SR, et al. Regulation of synaptic inputs to paraventricular-spinal output neurons by α2 adrenergic receptors. J Neurophysiol 2005; 93:393–402.

52 Greer SM, Trujillo AJ, Glover GH, et al. Control of nucleus accumbens activity with neurofeedback. Neuroimage 2014; 96:237–44.

53 Antelman SM, Caggiula AR. Norepinephrine-Dopamine Interactions and Behavior. 1977; 195:646–53.

54 Sara SJ. The locus coeruleus and noradrenergic modulation of cognition. Nat Rev Neurosci 2009; 10:211–23.

55 Espana RA, Berridge CW. Organization of Noradrenergic Efferents to Arousal-Related Basal Forebrain Structures. J Comp Neurol 2006; 496:668–83.

56 Mejías-Aponte CA, Drouin C, Aston-Jones G. Adrenergic and noradrenergic innervation of the midbrain ventral tegmental area and retrorubral field: Prominent inputs from medullary homeostatic centers. J Neurosci 2009; 29:3613–26.

57 Liprando LA, Miner LH, Blakely RD, et al. Ultrastructural Interactions between Terminals Expressing the Norepinephrine Transporter and Dopamine Neurons in the Rat and Monkey Ventral Tegmental Area. Synapse 2004; 52:233–44.

58 Wang CA, Munoz DP. A circuit for pupil orienting responses: Implications for cognitive modulation of pupil size. Curr Opin Neurobiol 2015; 33:134–40.

59 Strauch C, Wang CA, Einhäuser W, et al. Pupillometry as an integrated readout of distinct attentional networks. Trends Neurosci 2022; 45:635–47.

60 Zhu J, Iba M, Rajkowski J, et al. Projection from the orbitofrontal cortex to the locus coeruleus in monkeys revealed by anterograde tracing. Society for Neuroscience Abstracts 2004. p. 211–3.

61 Gilzenrat MS, Nieuwenhuis S, Jepma M, et al. Pupil diameter tracks changes in control state predicted by the adaptive gain theory of locus coeruleus function. Cogn Affect Behav Neurosci 2010; 10:252–69.

62 Murphy PR, Robertson IH, Balsters JH, et al. Pupillometry and P3 index the locus coeruleus-noradrenergic arousal function in humans. Psychophysiology 2011; 48:1532–42.

63 Hong L, Walz JM, Sajda P. Your eyes give you away: Prestimulus changes in pupil diameter correlate with poststimulus task-related EEG dynamics. PLoS One 2014; 9.

64 Mather M, Huang R, Clewett D, et al. Isometric exercise facilitates attention to salient events in women via the noradrenergic system. Neuroimage 2020; 210:116560.

65 Malik M, Task Force of the European Society of Cardiology the North American Society and the North American Society of Pacing Electrophysiology. Heart Rate Variability: Standards of Measurement, Physiological Interpretation, and Clinical Use. Circulation 1996; 93:1043–65.

66 Mihelj E, Bächinger M, Kikkert S, et al. Mental individuation of imagined finger movements can be achieved using TMS-based neurofeedback. Neuroimage 2021; 242:118463.

67 Zotev V, Krueger F, Phillips R, et al. Self-regulation of amygdala activation using real-time FMRI neurofeedback. PLoS One 2011; 6.

68 Hayes TR, Petrov AA. Mapping and correcting the influence of gaze position on pupil size measurements. Behav Res Methods 2016; 48:510–27.

69 Ehlers J, Georgi J, Huckauf A. Improving voluntary pupil size changes for HCI. Proceedings of the 8th International Conference on Pervasive Computing Technologies for Healthcare ICST; 2014. p. 343–6.

70 Bremner FD. Pupillometric evaluation of the dynamics of the pupillary response to a brief light stimulus in healthy subjects. Investig Ophthalmol Vis Sci 2012; 53:7343–7.

71 Miles WR. Ocular dominance in human adults. J Gen Psychol 1930; 3:412–30.

72 Kret ME, Sjak-Shie EE. Preprocessing pupil size data: Guidelines and code. Behav Res Methods Springer New York LLC; 2018; 51:1136–342.

73 Mathôt S, Fabius J, Heusden E Van, et al. Safe and sensible preprocessing and baseline correction of pupil-size data. Behav Res Methods 2018; 50:94–106.

74 Pataky TC, Vanrenterghem J, Robinson MA. Zero- vs. one-dimensional, parametric vs. non-parametric, and confidence interval vs. hypothesis testing procedures in one-dimensional biomechanical trajectory analysis. J Biomech Elsevier; 2015; 48:1277–85.

75 Pataky TC, Robinson MA, Vanrenterghem J. Vector field statistical analysis of kinematic and force trajectories. J Biomech Elsevier; 2013; 46:2394–401.

76 Behar JA, Rosenberg AA, Weiser-Bitoun I, et al. PhysioZoo: A novel open access platform for heart rate variability analysis of mammalian electrocardiographic data. Front Physiol 2018; 9:1–14.

77 Hill LBK, Siebenbrock A, Sollers JJ, et al. Are all measures created equal? Heart rate variability and respiration. 46th Annual Rocky Mountain Bioengineering Symposium and 46th International ISA Biomedical Sciences Instrumentation Symposium 2009 2009. p. 71–6.

78 Munoz ML, Van Roon A, Riese H, et al. Validity of (Ultra-)Short recordings for heart rate variability measurements. PLoS One 2015; 10:1–15.

79 Thong T, Li K, McNames J, et al. Accuracy of Ultra-Short Heart Rate Variability Measures. Annual International Conference of the IEEE Engineering in Medicine and Biology - Proceedings 2003. p. 2424–7.

80 Korn CW, Bach DR. A solid frame for the window on cognition: Modeling event- related pupil responses. J Vis 2016; 16:1–16.

81 Faull OK, Jenkinson M, Ezra M, et al. Conditioned respiratory threat in the subdivisions of the human periaqueductal gray. Elife 2016; 5:1–19.

82 Smith SM. Fast robust automated brain extraction. Hum Brain Mapp 2002; 17:143–55.

83 Jenkinson M, Bannister P, Brady M, et al. Improved optimization for the robust and accurate linear registration and motion correction of brain images. Neuroimage 2002; 17:825–41.

84 Woolrich MW, Ripley BD, Brady M, et al. Temporal Autocorrelation in Univariate Linear Modeling of FMRI Data. Neuroimage 2001; 14:1370–86.

85 Brooks J, Faull O, Pattinson K, et al. Physiological Noise in Brainstem fMRI. Front Hum Neurosci 2013; 7.

86 Glover GH, Li TQ, Ress D. Image-based method for retrospective correction of physiological

motion effects in fMRI: RETROICOR. Magn Reson Med 2000; 44:162–7.

87 Smith SM, Jenkinson M, Woolrich MW, et al. Advances in functional and structural MR image analysis and implementation as FSL. Neuroimage 2004; 23:208–19.

88 Griffanti L, Douaud G, Bijsterbosch J, et al. Hand classification of fMRI ICA noise components. Neuroimage 2017; 154:188–205.

89 Jenkinson M, Smith S. A global optimisation method for robust affine registration of brain images. Med Image Anal 2001; 5:143–56.

90 Greve DN, Fischl B. Accurate and robust brain image alignment using boundary-based registration. Neuroimage Elsevier Inc.; 2009; 48:63–72.

91 Andersson JLR, Jenkinson M, Smith S. Non-linear registration, aka spatial normalization (FMRIB technical report TR07JA2). 2007.

92 Woolrich MW, Behrens TEJ, Smith SM. Constrained linear basis sets for HRF modelling using Variational Bayes. Neuroimage 2004; 21:1748–61.

93 Wall MB, Walker R, Smith AT. Functional imaging of the human superior colliculus: An optimised approach. Neuroimage 2009; 47:1620–7.

94 Woolrich MW, Behrens TEJ, Beckmann CF, et al. Multilevel linear modelling for FMRI group analysis using Bayesian inference. Neuroimage 2004; 21:1732–47.

95 Bakdash JZ, Marusich MLR. Package ‘rmcorr .’ 2021; .